

# Towards 1 Gbps/UE in Cellular Systems: Understanding Ultra-Dense Small Cell Deployments

David López-Pérez<sup>1</sup>, Ming Ding<sup>2</sup>, Holger Claussen<sup>1</sup>, and Amir H. Jafari<sup>1,3</sup>

<sup>1</sup> Bell Laboratories, Alcatel-Lucent, Republic of Ireland

<sup>2</sup> National ICT Australia (NICTA), Australia

<sup>3</sup> University of Sheffield, United Kingdom

**Abstract**—Today’s heterogeneous networks comprised of mostly macrocells and indoor small cells will not be able to meet the upcoming traffic demands. Indeed, it is forecasted that at least a  $100\times$  network capacity increase will be required to meet the traffic demands in 2020. As a result, vendors and operators are now looking at using every tool at hand to improve network capacity. In this epic campaign, three paradigms are noteworthy, i.e., network densification, the use of higher frequency bands and spectral efficiency enhancement techniques. This paper aims at bringing further common understanding and analysing the potential gains and limitations of these three paradigms, together with the impact of idle mode capabilities at the small cells as well as the user equipment density and distribution in outdoor scenarios. Special attention is paid to network densification and its implications when transitioning to ultra-dense small cell deployments. Simulation results show that network densification with an average inter site distance of 35 m can increase the cell-edge UE throughput by up to  $48\times$ , while the use of the 10 GHz band with a 500 MHz bandwidth can increase the network capacity up to  $5\times$ . The use of beamforming with up to 4 antennas per small cell base station lacks behind with cell-edge throughput gains of up to  $1.49\times$ . Our study also shows how network densifications reduces multi-user diversity, and thus proportional fair alike schedulers start losing their advantages with respect to round robin ones. The energy efficiency of these ultra-dense small cell deployments is also analysed, indicating the need for energy harvesting approaches to make these deployments energy-efficient. Finally, the top ten challenges to be addressed to bring ultra-dense small cell deployments to reality are also discussed.

**Index Terms**—Macrocell, small cell, ultra-dense deployment, densification, frequency, antenna, interference, capacity, energy, cost-effectiveness.

## I. INTRODUCTION

“As old as I have become, many developments my eyes have seen. When I was a young man, changes used to take place from time to time, every now and then. Nowadays, they occur every so often ... life itself seems to change every day.” – a 97-years-old man commented, making reference to the increasing pace in the development of communication systems and applications through the last century.

These comments may seem exaggerated at first sight, but they may not be so, in light of the advancements seen in the telecommunication industry since Graham Bell carried out the first successful bi-directional telephone transmission in 1876 [1]. In this period of time, society has witnessed long distance communications being freed from wires and being operated through air at the speed of light; wireless and mobile communications made available to over 6 billion

users worldwide [2]; new types of communications and social interactions are emerging through the Internet and social networking [3] [4]; and many other breakthroughs that have certainly changed our every day lives.

These developments, although of great importance to the 97-years-old man, will probably appear as small steps towards a new era to future generations. This new era of communications, still in its first infancy, will continue to change the world in unpredictable and fascinating manners.

Even though there is uncertainty on how such future advancements will look like, it is expected that they follow the same trends as previous communication systems and technology breakthroughs, and they require more and more capacity, bits per second (bps), as time goes by. Voice services [5] were the killer applications at the beginning of this century, demanding tens of kbps per User Equipment (UE), while high quality video streaming [6] is the most popular one today, needing tens of Mbps per UE [7]. Future services such as augmented reality, 3D visualisation and online gaming may use multiple displays requiring hundreds of Mbps each, resulting in total sum of up to 1 Gbps per UE, and who knows what else tomorrow will bring?

In view of such significant future traffic demands, the mobile industry has set its targets high, and has decided to improve the capacity of today’s networks by a factor of  $100\times$  or more over the next 20 years –  $1000\times$  the most ambitious [8].

In order to achieve this goal, vendors and operators are currently looking at using every tool they have at hand, where the existing tools can be classified within the following three paradigms as illustrated in Fig. 1:

- Enhance spatial reuse through network densification, i.e., Heterogeneous Networks (HetNets) and small cells [9] [10] [11] [12].
- Use of larger bandwidths, exploiting higher carrier frequencies, both in licensed and unlicensed spectrum [13] [14] [15].
- Enhance spectral efficiency through multi-antenna transmissions [16], cooperative communications [17], dynamic TDD techniques [18] [19] [20], etc.

This toolbox provides vendors and operators with choice and flexibility to improve network capacity, but leads to new enigmas on how each operator should make the investment to meet the capacity demands. Different operators with different

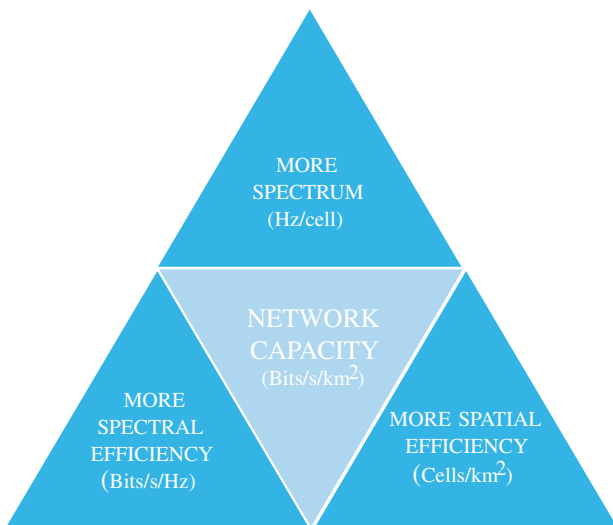


Fig. 1. Existing paradigms to improve network capacity: more spectrum, more spectral efficiency and more spatial efficiency.

financial means, customer market segmentation, existing network assets and technical expertise may require different solutions. Network densification complicates network deployment as well as backhauling and mobility management, while higher carrier frequencies suffer from larger path losses, and usually require more expensive equipment. Most spectral efficiency enhancement technologies depend on a tight synchronisation as well as relatively complex signal processing capabilities, and may be compromised due to inaccuracies in Channel State Information (CSI). Capital Expenditure (CAPEX) and Operational Expenditure (OPEX) are also major concerns since the price per bit should be kept at minimum. To make things more complex, network deployments strategies should consider that these three paradigms have their own fundamental limitations and thus cannot be infinitely exploited. Finding the right portfolio of tools to meet the key requirements is vital for both vendors and operators.

In this light, this paper aims at bringing further common understanding and analysing the potential gains and limitations of network densification, in combination with the use of higher frequency bands and spectral efficiency enhancement techniques. The impact of idle mode capabilities at the small cells as well as UE density and distribution are also studied since they are foreseen to have a large impact [21]. The objective of this paper is to shed new light on the Pareto set of network configurations in terms of small cell density, frequency band of operation and number of antennas per small cell Base Station (BS) that can meet future traffic demands, achieving an average throughput exceeding 1 Gbps per UE.

The rest of the paper is organised as follows: Section II addresses the important roles of small cells, and depicts our view on future small cell deployments HetNets. Section III presents the state of the art of current small cell technologies together with its drawbacks, and motivates the need for uncoordinated dense small cell deployments. Section IV presents the system model to be used in this paper to analyse ultra-dense small cell deployments. Sections V, VI and VII elaborate on the three paradigms to enhance network performance, i.e., network den-

sification together with the usage of higher carrier frequencies and multi-antenna transmissions, respectively. Section VIII investigates the impact of network densification in small cell BS schedulers. Section IX studies the impact of network densification on the energy efficiency. Section X highlights the main differences between regular HetNets and ultra-dense HetNets, while Section XI summarises the challenges in ultra-dense small cell deployments. Finally, Section XII draws the conclusions.

## II. SMALL CELLS IN HETNETS

Given the different approaches to enhance network capacity, it may be worth understanding how network capacity has been improved in the past and which have been the lessons learnt to make sure the best choices are taken. To this end, Prof. Webb analysed the different methods used to enhance network capacity from 1950 to 2000 [22]. According to his study, the wireless capacity has increased around a 1 million fold in 50 years. The breaking down of these gains is as follows:  $15\times$  improvement was achieved from a wider spectrum,  $5\times$  improvement from better Medium Access Control (MAC) and modulation schemes,  $5\times$  improvement by designing better coding techniques, and an astounding  $2700\times$  gain through network densification and reduced cell sizes. According to this data, it seems obvious that if we are looking for a  $1000\times$  improvement in network performance, network densification through ultra-dense small cell deployments is the most appealing approach, and today's networks have already started going down this path.

In order to meet the exponentially increasing traffic demands [23], mobile operators are already evolving their networks from the traditional macrocellular-only networks to HetNets [24], [25], in which small cells reuse the spectrum locally and provide most of the capacity while macrocells provide a blanket coverage for mobile UEs. Currently, small cells are deployed in large numbers. Indeed, according to recent surveys, in 2012, the number of small cell BS was already larger than that of macrocell BSs [26]. These small cell deployments are mainly in the form of home small cells, known as femtocells [11], [27], [28], but many operators have also already started to deploy outdoor small cell solutions to complement their macrocellular coverage [29].

Most of the existing small cell deployments, particularly femtocells, are configured to transmit on a dedicated carrier different from that of the macrocells [27]. While this avoids inter-tier interference, it also limits the available radio spectrum that each cell can access, and is less efficient than co-channel deployments, in which small cells and macrocells share the same frequency bands [30]. However, while co-channel operation provides better frequency utilisation, the additional inter-tier interference can result in coverage and handover issues for mobile UEs [31] [32]. This interference issue is particularly severe in femtocell deployments with Closed Subscriber Group (CSG) access, in which UEs cannot connect to the strongest cell; the later thus becoming a strong interferer [31].

In order to take advantage of the benefits of both orthogonal and co-channel network deployments – interference mitigation

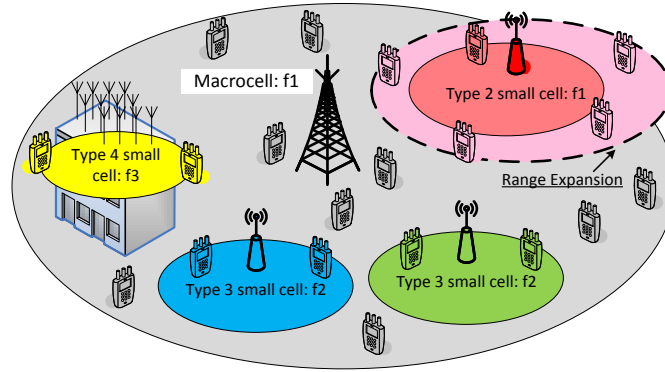


Fig. 2. Cell tier types.

TABLE I  
CELL TIER TYPES AND THEIR CHARACTERISTICS.

Cell Type No.	Cell Type	Spectrum	Relationship with the Macrocell Tier	Typical Use Case
1	low-frequency macrocell tier	around 1~2GHz, licensed	-	umbrella coverage
2	low-frequency small cell tier	around 1~2GHz, licensed	co-channel deployment, CRE & ABS	capacity enhancement in hotspots
3	mid-frequency small cell tier	around 5GHz, unlicensed	non-co-channel deployment, dual connectivity	high traffic offloading
4	high-frequency small cell tier	>10GHz, unlicensed	non-co-channel deployment, dual connectivity	very high traffic offloading

and spectrum reuse, respectively – and further enhance the capacity of future networks, we anticipate that future networks will be comprised of different small cell tiers with different types of small cell BSs. These different types of small cell BSs will be targeted at different types of environments and traffic. Fig. 2 and Table I summarises our classification of future network tiers. Note, that to make the framework more complete, we treat the macrocell tier as a special case of the small cell tiers in Table I.

*Cell Type 1* is essentially the conventional macrocell tier that provides an umbrella coverage for the network. This topic will not be covered in this paper since it is out of our scope. However, it is important to mention that a noteworthy enhancement for Cell Type 1 that is currently being investigated is the 3-Dimensional (3D) Multi-User (MU) Multiple Input Multiple Output (MIMO) transmission, which is expected to enhance the indoor penetration and spectral efficiency of macrocells, especially for the scenario with high-rise buildings [33] [34].

*Cell Type 2* features today’s state of the art co-channel deployments of small cells with the macrocell tier. Cell Type 2 is conceived as an add-on to Cell Type 1 for capacity enhancement through cell splitting gains in hotspots. Long Term Evolution (LTE) Release 10 features such as Cell-Specific Reference Symbol (CRS) and enhanced Inter-cell Interference Coordination (eICIC) are critical for this small cell type to provide efficient macrocell off-loading and cope with the inter-tier interference issue [25]. Besides, advanced receivers with interference cancellation capabilities are an enhancement for small cell UEs to remove the residual interference from CRS [35]. Moreover, multi-cell cooperation among nodes with different power levels has been proved to be beneficial in recent works [36] [37]. The eICIC and another important characteristics such as Cell Range Expansion (CRE) and Almost Blank Subframe (ABS) of Cell Type 2 will be introduced in

the following section, together with its drawbacks and need for new cell types.

*Cell Type 3* features dense orthogonal deployments of small cells with the macrocell tier, which are envisaged to be the workhorse for network capacity boosting through extensive spatial reuse in the near future. Due to its small size, Cell Type 3 is not appropriate to support mobile UEs and is targeted at static UEs, which represent a vast majority of the UE population with more than 80% of today’s data traffic carried indoors [38]. In order to ensure a smooth inter-working between Cell Type 3 and Cell Type 1, Dual Connectivity (DC) is a promising technology currently being investigated in the LTE framework [39]–[42], where a given UE may use radio resources provided by at least two different network points (Master and Secondary BSs) connected with non-ideal backhaul. The typical usage of DC is the splitting of traffic flows [43]. In more detail, it is beneficial to let macrocells provide the voice service for a UE and outsource the UE’s data service to small cells. In addition, DC also improves the robustness of the mobility management since UEs are now connected to two cell tiers [43]. Note that DC is not suitable for Cell Type 2 because its compatibility with eICIC is challenging. In essence, eICIC tries to make macrocells invisible to small cell UEs in certain subframes using the ABS mechanism to eliminate the inter-tier interference. On the other hand, DC tries to maintain both connections, one to the macrocells and one to the small cells. Hence, eICIC is mainly used in the co-channel deployment where the macrocell to small cell interference is a major issue, while DC is mainly suitable for the orthogonal deployment where the traffic flow splitting or the mobility management is a major issue. Other new emerging technologies in Cell Type 3 include dynamic small cell idle modes [21] [44] [45], dynamic Time Division Duplexing (TDD) transmission [18] [19] [20] (which have attracted a

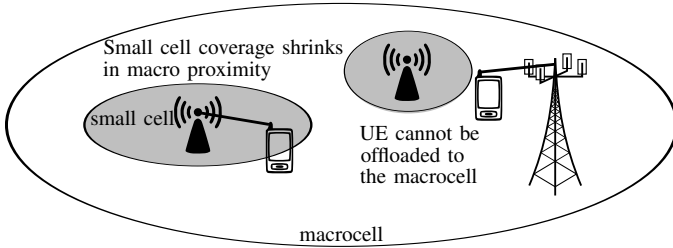


Fig. 3. Small cell coverage shrinks in the proximity of a macrocell BS leading to poor offloading.

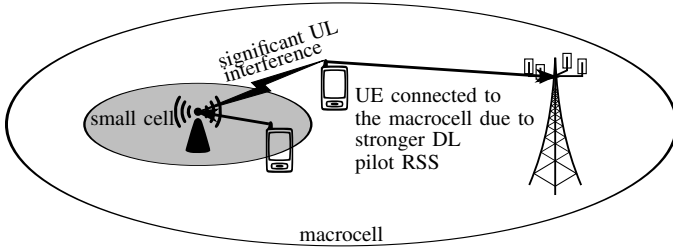


Fig. 4. Macrocell UE jamming the UL of a nearby small cell.

lot of momentum in both the academia and the industry in the last years), high-order MIMO techniques [46] [47], etc.

*Cell Type 4*, finally, will push the technology frontier even further by using a very wide spectrum in high-frequency bands, e.g., mmWave [48] [49] [50], and exploiting massive MIMO techniques to achieve large beam forming and spatial multiplexing [51] [52], etc.

### III. WHY ARE TODAY'S SMALL CELLS NOT PRACTICAL TO MEET FUTURE CAPACITY DEMANDS?

In contrast to CSG, open access helps to minimise inter-tier interference since UE are always allowed to connect to the strongest cell, thus avoiding the CSG interference issue [31]. However, in a co-channel deployment of small cells with the macrocell tier, being attached to the cell that provides the strongest pilot Reference Signal Strength (RSS) may not be the best strategy since UEs will tend to connect to macrocells rather than to small cells, even if they are at a shortest path loss distance. This is due to the large difference in transmission power between both types of BSs. As shown in Fig. 3, the closer the small cell BS is to the macrocell BS, the smaller the small cell coverage is due to macrocell BS power dominance. This results in a poor macrocell off-load [24] [25]. Moreover, due to this server selection procedure based on pilot RSS, UEs connected to macrocells will also severely interfere with all small cells located in their vicinity in the UL. This is shown in Fig. 4. Note that due to the lower path loss, if a macrocell UE would connect to the small cell with the smallest path loss, this UE would transmit with a much lower Uplink (UL) power. This would allow load balancing as well as UL interference mitigation, thus improving network performance.

In order to address these problems arising from the significant power difference between co-channel BSs in HetNets,

new cell selection methods that allow UE association with cells that do not necessarily provide the strongest pilot RSS are necessary. In this regard, CRE has been proposed in the 3rd Generation Partnership Project (3GPP) for increasing the Downlink (DL) coverage footprint of small cells by adding a positive cell individual offset to the pilot RSS of the small cells during the serving cell selection procedure [53] [29]. CRE mitigates UL interference and facilitates offloading. With a larger Range Expansion Bias (REB), more UEs are offloaded to the small cells, at the cost of increased co-channel DL interference for the range-expanded UEs (see Fig. 5). Without Inter-cell Interference Coordination (ICIC), range-expanded UEs are not connected anymore to the strongest cell, CRE has been shown to degrade the throughput of the overall network but improve the sum capacity of the macrocell UEs due to offloading. In [54], closed form analytical expressions of outage probability with CRE in HetNets corroborate that CRE without ICIC degrades the outage probability of the overall network.

In order to address this issue, the use of eICIC schemes has been proposed to guarantee the proper operation of CRE [24] [25]. In such schemes, special attention is given to the mitigation of inter-cell interference in the control channels transmitted in the DL. UEs may declare radio link failure under severe interference, and experience service outage due to the unreliable control channels.

Among the proposed eICIC schemes, time-domain eICIC methods have received a lot of attention, particularly ABSs [55]. In an ABS, no control or data signals but only reference signals are transmitted, thus significantly mitigating interference since reference signals only occupy a very limited portion of the whole subframe. As shown in Fig. 6, ABSs can be used to mitigate interference problems in open access small cells that implement CRE. A macrocell can schedule ABSs while small cells can schedule its range-expanded small cell UEs within the subframes that are overlapping with the macrocell ABSs. ABSs can also be used to mitigate interference problems in CSG small cells. CSG small cells can schedule ABSs while macrocells can schedule their victim macrocell UEs located nearby a CSG small cell within the subframes that are overlapping with the small cell ABSs. Moreover, ABSs can be scheduled at the small cell BS to allow fast moving macrocell UEs to move through it. In order to minimise the capacity loss at the BSs scheduling ABSs, the agreement in [56] generalises ABSs from completely blank data and control symbols to the transmission of such symbols at a reduced-power level, implying that the aggressing BS may also be able to transmit information. In [57], the network performance improvement due to CRE and ABSs was analysed showing the merits of ABSs. Moreover, analytic expressions for average capacity and 5th percentile throughput were derived in [58], while considering ABSs and power reduced subframes as a function of BS densities, transmit powers and interference coordination parameters in a two-tier HetNet scenario. The results confirm the benefits of power reduced subframes over ABSs.

In order to enable efficient interference mitigation, however, REB and ABS schemes (reduced power subframes also

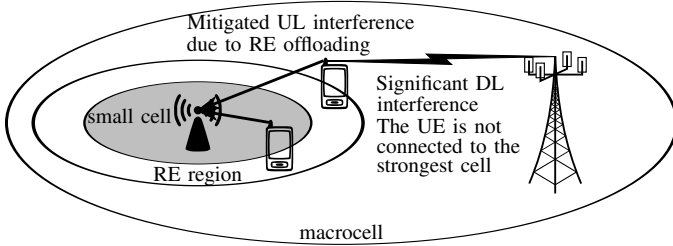


Fig. 5. Range expansion mitigates UL interference and facilitates offloading at the expense of increasing DL interference.

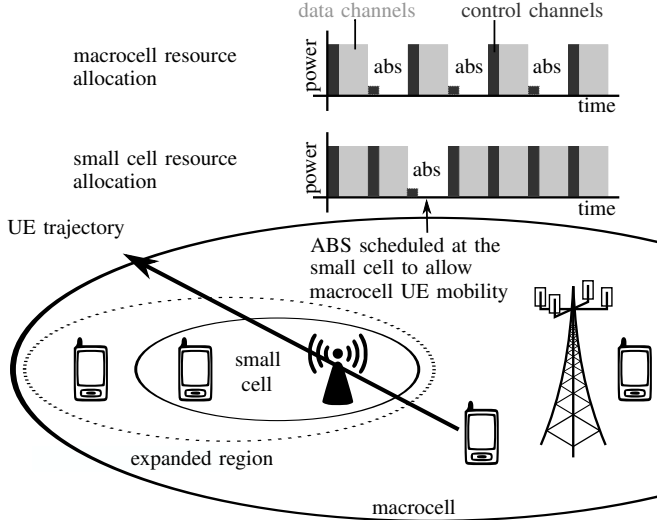


Fig. 6. ABS concept. ABS scheduled at the macro BS to help pico range-expanded UEs. ABS scheduled at small cells to help mobile macro UEs.

included in this category) should be able to dynamically adapt to the number of small cells at various geographical locations and different traffic conditions. The larger the REB for a given small cell BS, the more expanded-region Picocell User Equipments (PUEs) connect to it, and thus a larger macrocell ABS duty cycle (ratio of ABS to non-ABSs) is needed to provide a desired quality of service to these expanded-region PUEs. In contrast, the larger the ABS duty cycle, the lower the macrocell performance may be due to subframe blanking. A dynamic adaptation of ABS patterns can be realised through X2 backhaul inter-BS coordination, where neighbouring macrocell BSs agree on a given ABS pattern, and then each macrocell BS informs its overlaid small cells BSs of which subframes it will use for scheduling Macrocell User Equipments (MUEs) and which ones will be blanked for interference mitigation. In [59], a mathematical framework to efficiently compute UE association and corresponding REBs together with ABS duty cycles is proposed. The solution is provably within a constant factor of the optimal solution, scales linearly with the number of cells and is also amenable to distributed optimisation. However, it requires extensive input information from each UE with respect to its best macrocell and small cell BSs, which may be difficult to obtain since a

UE cannot be simultaneously connected to multiple cells.

In addition, for an efficient interference mitigation, inter-macrocell BS coordination should be considered [60]. If neighbouring macrocells do not coordinate their ABS patterns and they are not fully time aligned, this will cause additional interference fluctuations in the network, resulting in less efficient link adaptation and radio-aware packet scheduling.

From the previous discussion, it can be derived that a joint optimisation of REBs, ABS patterns, power reduction factors in reduced power subframes, scheduling thresholds and frequent inter-BS coordination may be required to achieve a good performance in a co-channel deployment of small cells with the macrocell tier. The complexity of these optimisation procedures will be aggravated with the number of cells, and thus we anticipate that Cell Type 2 is not suitable for ultra-small cell deployments, where network planning should be completely avoided. This suggests that co-channel deployments of small cells with the macrocell tier should be aimed at hotspot locations with a reasonable low number of small cells (less than 10 per macrocell sector), while ultra-dense deployments should use dedicated carriers to circumvent interference problems and the planning stage. This gives rise to Cell Type 3, the focus of this paper.

#### IV. SYSTEM MODEL

Due to the insufficient capacity provided by Cell Type 1 and 2 to meet the forecasted mobile traffic demands, in this paper, our focus is on Cell Type 3, i.e., non-co-channel mid-frequency small cell deployments with the macrocell tier. This cell type has the potential to significantly enhance network performance through a high network densification and the usage of relatively high frequency bands, while avoiding interference and coordination issues with the macrocell tier, designed to support fast moving UEs. The relatively small size of antennas at mid-frequency bands around 10 GHz is also an appealing feature in order to exploit multi-antenna transmission technique gains.

In the following, our system model to analyse ultra-dense small cell networks is introduced.

Consider a dense network of small cells. In this system model, a 500-by-500m scenario is used, and small cells are placed outdoors in a uniform hexagonal grid with different Inter Site Distances (ISDs) of 200, 150, 100, 75, 50, 35, 20, 10 or 5 m, which result in 29, 52, 116, 206, 462, 943, 2887, 11548 or 46189 small cell BSs per square km deployed in the scenario, respectively.

Two scenarios for UE distribution are considered, with three different UE densities of 600, 300 or 100 active UEs per square km:

- Uniform: UEs are uniformly distributed within the scenario.
- Non-uniform: Half of the UEs are uniformly distributed within the scenario, while the other half are uniformly distributed within circular hot spots of 40 m radius with 20 UEs each. Hot spots are uniformly distributed, and the minimum distance between two hotspot centres is 40 m.

Note that 300 active UEs per square km is the density usually considered in dense urban scenarios, such as Manhattan [61].

In terms of frequency bands, four carrier frequencies are considered, i.e., 2.0, 3.5, 5.0 and 10 GHz, where the available bandwidth is 5 % of the carrier frequency, i.e., 100, 175, 250 and 500 MHz, respectively.

In terms of antennas implementation and operation, each small cell BS has 1, 2, or 4 antennas deployed in a horizontal array (see Fig. 18), while the UE has only 1 antenna. The standardised LTE code book beamforming is adopted, targeted in this case at maximising the received signal strength of the intended UE (quantised Maximal Ratio Transmission (MRT) beamforming with no inter-BS coordination required). It is important to note that the power per antenna remains constant and that beamforming is only applied to the data channels and not to the control channels, which define the small cell coverage,

The transmit power of each active BS is configured such that it provides a Signal to Noise Ratio (SNR) of 9, 12 or 15 dB at the targeted coverage range, which is  $\frac{\sqrt{3}}{2}$  of the ISD [27].

UEs are not deployed within a 0.5 m range of any BS, and all UEs are served by the BS from which they can receive the strongest received pilot signal strength, provided that the pilot Signal to Interference plus Noise Ratio (SINR) is larger than -6.5 dB.

A BS with no associated UE is switched off. This is the idle mode capability presented in [62], and adopted in this paper.

With regard to scheduling, we envision that because of the use of mid- to high-frequency bands and due to the importance of the Line Of Sight (LOS) component in small cells, the time spread of the Channel Impulse Response (CIR) will be very small, typically in the order of several  $\mu$ s, and hence the impact of multi-path fading will become less significant in the future. Therefore, multi-path fading is not considered in our analysis, and a round robin scheduler designed for simple implementation is adopted. This argument is supported by the analysis in Section VIII, where the impact of network densification in small cell BS schedulers is investigated [63].

For details on path loss, antenna gain, shadow fading, SINR computation and capacity mapping, please refer to Appendix A. The modelling of multi-path fast fading for the analysis in Section VIII is presented in Appendix A.

For the sake of clarity, it is also important to mention that in the legend of the figures of this paper,  $i$  indicates the ISD of the scenario in meter,  $d$  indicates the density of UEs per square km,  $ud$  indicates the UE distribution ( $ud = 0$  uniform;  $ud = 1$  non-uniform)  $s$  indicates whether the idle mode capability of the small cell BS is activated or deactivated,  $sm$  indicates the idle mode index of the idle mode used in the energy efficiency analysis,  $f$  indicates the carrier frequency in GHz  $a$  indicates the number of antennas, and  $t$  indicates the SNR target of the small cell BS at its cell-edge, which is located at  $\frac{\sqrt{3}}{2}$  of the ISD.

## V. NETWORK DENSIFICATION

Network densification has the potential to linearly increase the capacity of the network with the number of deployed cells through spatial spectrum reuse, and is considered to be the key enabler to provide most of the capacity gains in future networks.

In order to better understand the implications of network densification on network capacity, let us define network capacity based on the framework developed by Claude Shannon [64] as

$$C[\text{bps}] = \sum_m^M \sum_u^{U_m} B_{m,u}[\text{Hz}] \log_2(1 + \gamma_{m,u}[\cdot]), \quad (1)$$

where  $\{1, \dots, m, \dots, M\}$  is the set of BSs deployed in the network,  $\{1, \dots, u, \dots, U_m\}$  is the set of UEs connected to BS  $m$ ,  $B[\text{Hz}]$  is the total available bandwidth, and  $B_{m,u}[\text{Hz}]$  and  $\gamma_{m,u}[\cdot]$  are the bandwidth granted to and the SINR experienced by UE  $u$  when connected to BS  $m$ . This model assumes Gaussian interference.

At the network level, network densification increases the number of geographically separated BSs  $M$  that can simultaneously reuse the available bandwidth  $B$ , thus improving spatial reuse and linearly increasing network capacity with  $M$ .

At the cell level, a consequence of network densification is cell size reduction, which directly translates into a lower number of UEs  $U_m$  connected per BS  $m$  and thus a larger bandwidth  $B_{m,u}$  available per UE. In this way, network capacity linearly increases with the number of offloaded UEs.

Moreover, at the cell level too, the average distance between a UE and its serving BS reduces, while the distance to its interfering BSs does not necessarily reduce at the same pace assuming idle mode capabilities. This leads to an increased UE signal quality  $\gamma_{m,u}$ , and thus the network capacity logarithmically increases with the  $\gamma_{m,u}$ .

As can be derived from the above discussion, network densification increases  $M$  and in turn improves both  $B_{m,u}$  and  $\gamma_{m,u}$ , resulting in an increase of the capacity – see (1). However, the impact of UE density and distribution should not be forgotten. If network densification is taken to an extreme, and the number of deployed BSs is larger than the number of existing active UEs, this ultra-dense small cell deployment may reach a fundamental limit in which the number of active UEs per cell is equal or lower than one, i.e.,  $U_m \leq 1$ . At this point, the bandwidth  $B_{m,u}$  available per UE cannot be further increased through cell splitting, and thus network densification can only enhance network capacity at a lower pace in a logarithmic manner by bringing the network closer to the UE and improving the UE signal quality  $\gamma_{m,u}$ , which may not be as cost-effective. As a result, *one UE per cell* may be the operational sweet spot from a densification view point. In the following, we discuss the *one UE per cell* concept.

### A. Idle mode capability and the 1 UE per cell concept

One important advantage of having a surplus of cells in the network is that a large number of them could be switched off if there is no active UE within their coverage areas, which reduces interference to neighbouring UEs as well as energy consumption.

Provided that a surplus of cells exists and as a result of an optimal idle mode capability [62], the network would have the key ability of adapting the distribution of active BSs to the distribution of active UEs, and thus the number of active cells, transmit power of the network, and interference conditions would strongly depend on the UE density and distribution.

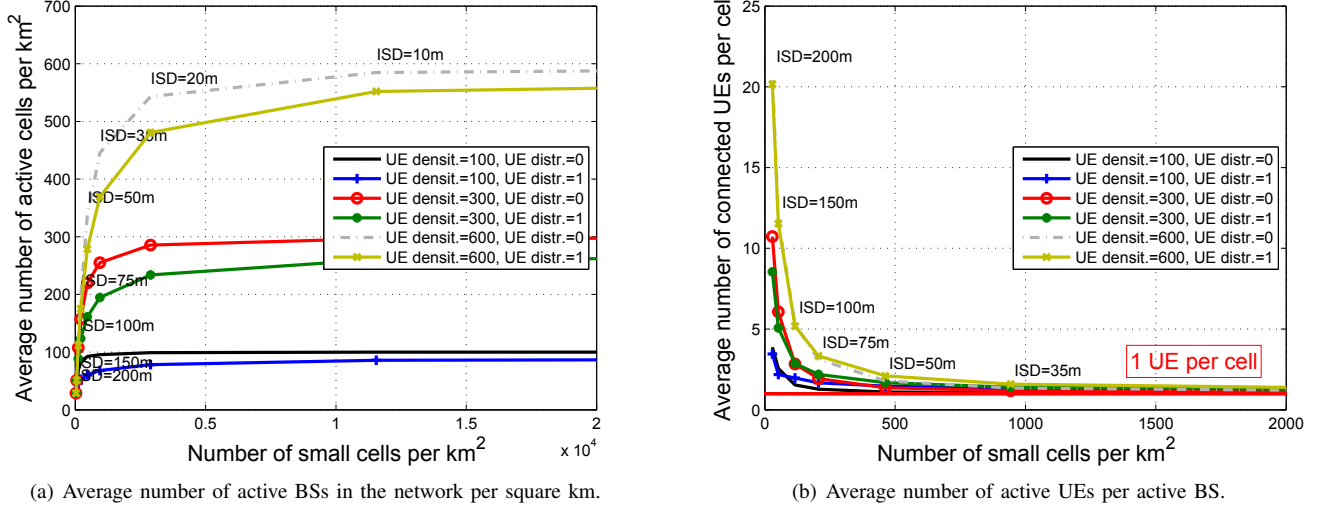


Fig. 7. Average number of active BSs in the network per square km and average number of active UEs per active BS. The UE densities are 600, 300 and 100 active UEs per km<sup>2</sup>. The UE distributions are uniform and non-uniform within the scenario. The rest of the parameters are  $s = 1$ ,  $f = 2$  GHz,  $\alpha = 1$  and  $t = 12$  dB.

According to our system model, Fig. 7 shows the average number of active BSs in the network per square km and the average number of active UEs per active BS, with the aforementioned idle mode capability (a BS with no associated UE is switched off). Different UE densities and distributions are considered. From Fig. 7(a), the following conclusions can be extracted. The lower the UE density, the lower the average number of active BSs in the scenario and the lower the average number of active UEs per active BS. With regard to UE distribution, a uniform distribution requires more active BSs than a non-uniform distribution to provide full coverage to a given UEs density. This is because UEs are more widely spread in the former. In contrast, due to the more active BSs, the uniform distribution results in a lower number of active UEs per active BS for a given UEs density, which tends to provide a better UE performance at the expense of an increased number of deployed active cells, and thus cost. This indicates the importance of understanding the UE density and distribution in specific scenarios to realise efficient deployments.

An important result that can be extracted from Fig. 7(b) is that an ISDs of 35 m can already achieve an average of 1.1 active UEs per active BS or smaller, approaching the fundamental limit of spatial reuse. Reaching such limit has implications for the network and UE performance, as it has been qualitatively explained before, and as it will be quantitatively shown in Section VI. Moreover, it also has implications for the cost-effectiveness of the deployment, since densifying further than the 1 UE per cell sweet spot requires an exponential increase in investment to achieve a diminishing logarithmic capacity gain through signal quality enhancement. In other words, when the network is dense enough, a large number of cells have to be added to the network to enhance the UE throughput in a noticeable manner, and this may not be desired since the operator may have to pay exponentially more money to carry on with the deployment.

### B. Transmit Power and UE SINR Distribution

Combining ultra-dense small cell deployments together with an efficient idle mode capability has the potential to significantly reduce the transmit power of the network. This is because active cells transmit to UEs with a lower power due to their reduced cell size and empty cells can be put into idle mode until a UE appears [62].

Moreover, by turning off empty cells, the interference suffered by UEs from always on channels, e.g., synchronisation, reference and broadcast channels, can also be removed, neutralising some neighbouring cells and thus improving UE SINR distributions.

Working in this direction, LTE Release 12 networks have defined periodic Discovery Reference Signals (DRSs) to facilitate UEs the discovery of small cells that are turned off [39]. DRSs are transmitted sparsely in the time domain and they consist of multiple types of Reference Signals (RSs), based on which UEs are able to perform synchronisation, detect cell identity and acquire coarse CSI, etc. Due to the low periodicity of DRSs, the impact of DRSs on UE SINR distribution is marginal, and thus it can be ignored.

1) *Transmit Power*: In terms of transmit power, Fig. 8(a) shows how the transmit power per active BS significantly reduces with the small cell BS density in the studied scenario. In this case, the transmit power of each active BS is configured such that it provides a SNR of 12 dB at the targeted coverage range, which is  $\frac{\sqrt{3}}{2}$  of the ISD. Note that here the required transmit powers are significantly lower compared to co-channel deployments where the small cells should exceed the received macrocell power in the intended coverage area. In addition, Fig. 8(b) shows how the overall transmit power used by the network also significantly reduces with the small cell BS density in the studied scenario, when the idle mode capability is considered. This is because the reduction of transmit power per cell outweighs the increased number of active cells,

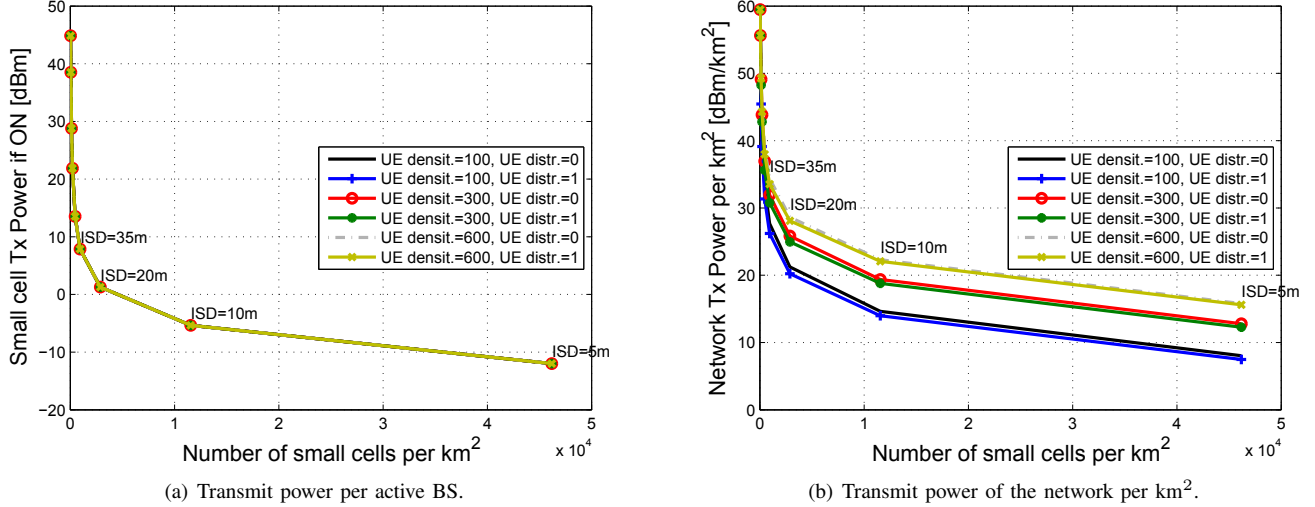


Fig. 8. Transmit power per active BS and transmit power of the network per km<sup>2</sup>. The UE densities are 600, 300 and 100 active UEs per km<sup>2</sup>. The UE distributions are uniform and non-uniform within the scenario. The rest of the parameters are  $s = 1$ ,  $f = 2$  GHz,  $a = 1$  and  $t = 12$  dB. It is important to note that in Fig. 8(a) there are 6 overlapping curves. This is because the power used by the cell if it is activated does not depend on the UE density.

and this fact holds true for both the uniform and non-uniform UE distribution, with network transmit power reductions of up to 43 dB. Note that this discussion only considers transmit powers, and that the overall power consumption of the network when considering the power consumed by the BSs in idle mode will be analysed in Section IX.

2) *UE SINR Distribution*: Traditional understanding has led to the conclusion that the UE SINR distribution and thus outage probability is independent of BS density. The intuition behind this phenomenon is that the increase in signal power is exactly counter-balanced by the increase in interference power, and thus increasing the number of BSs does not affect the coverage probability. This is a major result in the literature [65] [66], which only holds under the assumption of a single-slope path loss model more suited for rural areas. However, conclusions may be different for urban and dense urban scenarios where Non Line Of Sight (NLOS) to LOS transitions may occur.

In order to show this, Fig. 9 and Fig. 10 respectively show the SINR spatial distribution and UE SINR Cumulative Distribution Functions (CDFs) for several ultra-dense small cell deployments with different small cell densities with and without idle mode capability. Recall that our path loss models the NLOS to LOS transition with the probabilistic function defined for urban microcell environments in [67]. Let us now analyse the results.

When the idle mode capability is deactivated, our results show that the UE SINR CDF degrades with the small cell density, contradicting the results in [65] [66] where it is independent of BS density. As the network becomes denser, the ISD is reduced and the LOS component starts to dominate the path loss model for the interfering signals. While in traditional networks with large ISDs the carrier signal may be subject to LOS depending on the distance between the UE and its serving BS, the interfering signal is not usually subject to LOS due to the large distance between the serving BS and

its interfering BSs. However, with the smaller ISDs, LOS starts dominating the interfering signal too and this brings down the UE SINR, thus lowering the UE and cell throughputs. In other words, the interference power increases faster than the signal power with densification due to the transition of the former from NLOS to LOS, and thus the BS density matters! This new conclusion should significantly impact network deployment strategies, since the network capacity no longer grows linearly with the number of cells, based on previous understanding. Instead, it seems to increase at a lower pace as the BS density increases, and thus operators may find themselves paying exponentially more money for diminishing gains when heavily densifying their networks.

However, the good news is that when the idle mode capability is activated, the trend is just the opposite, and the UE SINR CDF is significantly boosted with the cell density as a result of interference mitigation. The denser the BS deployments, the larger the capacity increase, since more BS can be turned off, which reduces interference. When the ISD among BSs is 35 m, the median SINR improvement compared to the case when the idle mode capability is deactivated is around 8.76 dB, while for an ISD of 10 m the median SINR improvement is around 20.62 dB. This is a significant improvement.

As conclusion, it is important to note that an optimum idle mode capability not only plays a significant role in transmit power savings, but also as an interference mitigation technique.

### C. Transition from Interference to Noise Limited Scenarios

As shown in Fig. 7, in ultra-dense small cell deployments, a large number of cells should be switched off when the BS density is large and the UE density is low; this combination leads to the most effective interference mitigation. However, is this interference mitigation through small cell deactivation large enough to transition from an interference limited scenario



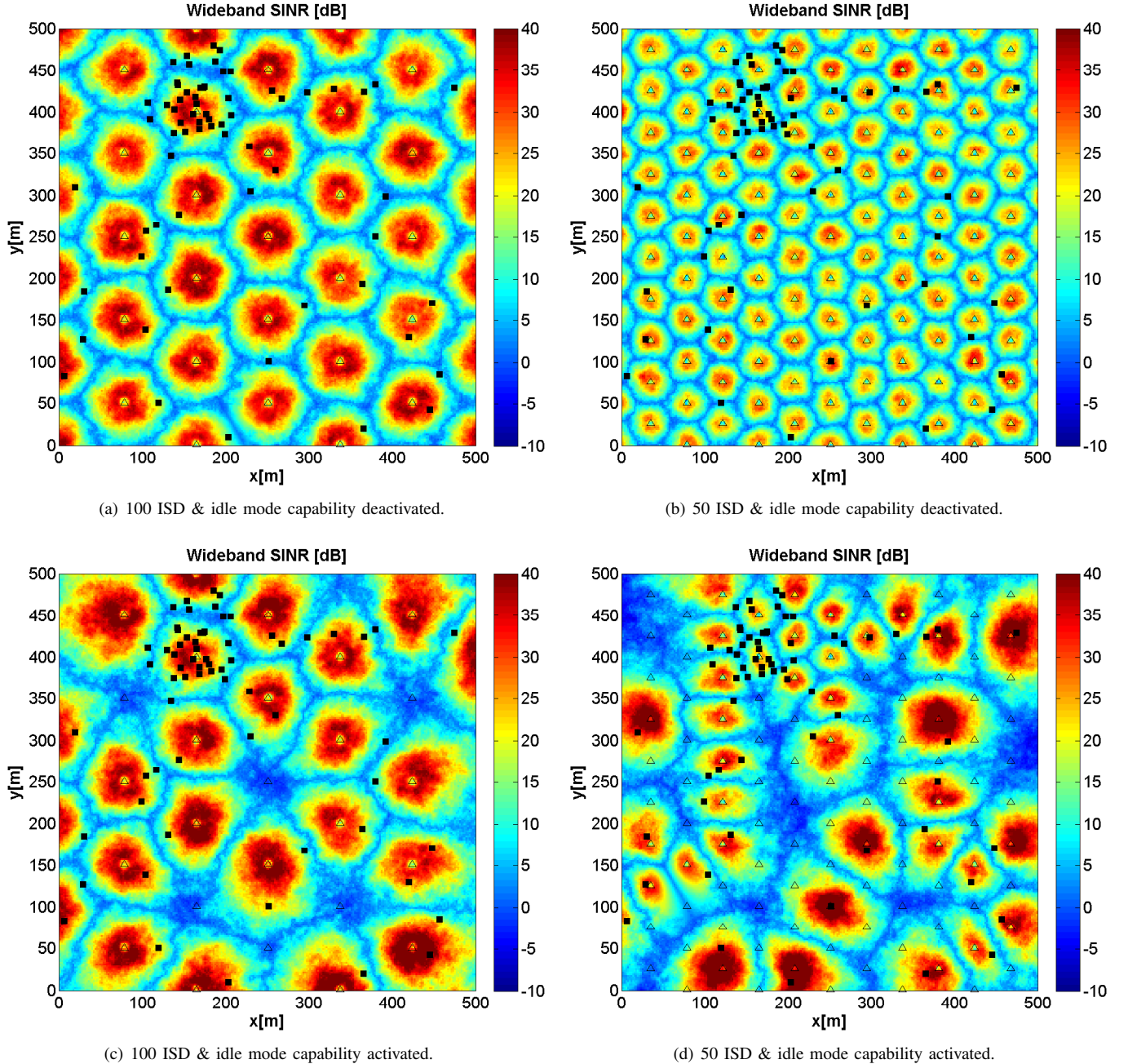


Fig. 9. SINR spatial distributions of several ultra-dense small cell deployments with ISD among small cell BSs of 100 and 50 m with or without idle mode capabilities. The rest of the parameters are  $d = 300 \text{ UE/km}^2$ ,  $ud=1$ ,  $s = 1$ ,  $f = 2 \text{ GHz}$ ,  $a = 1$  and  $t = 12 \text{ dB}$ . The triangles represent BSs and the squares represent UEs.

to a noise limited scenario? In an interference limited scenario, the signal quality of a UE is independent of the transmit power of the serving and the interfering BSs, provided that they all use the same transmit power. However, this is not the case in a noise limited scenario where the signal quality of a UE improves with the transmit power of the serving BS, as the noise remains constant. Therefore, if such transition takes place, the tuning of the small cell BS transmit power becomes even more important, since the transmit power will not only determine the coverage radius of the cell but will also affect the capacity of the network.

In order to answer this question, Fig. 11 shows the UE SINR CDF in different ultra-dense small cell deployments, while considering different transmit power for the small cell BSs. In more detail, the targeted SNRs at  $\frac{\sqrt{3}}{2}$  of the ISD are set to 9, 12 or 15 dB. Different UE densities are also considered, 100 and 600 UEs per square km. The results show that the change in transmit power only has an impact on the SINR distribution of the scenario with the larger BS densities, ISD=5 m and ISD=10 m, and the lowest UE densities, 100 active UEs per  $\text{km}^2$ . Otherwise, the SINR distribution is independent of the transmit power, indicating that this transition does

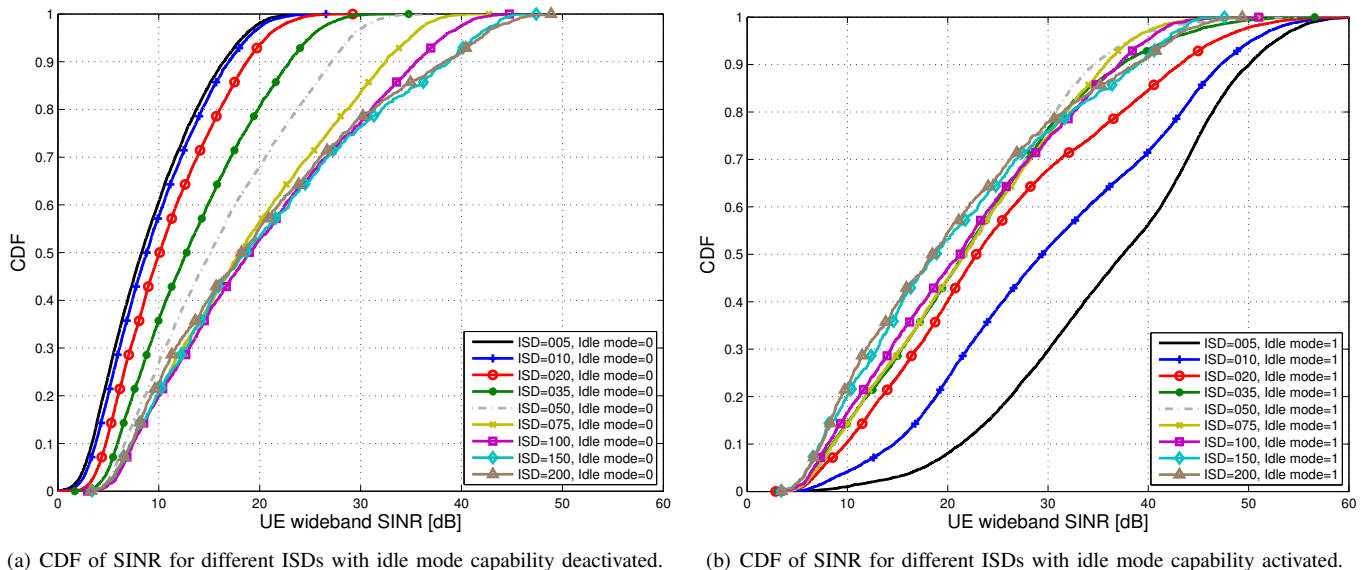


Fig. 10. UE SINR CDF of several ultra-dense small cell deployments with ISD among small cell BSs of 200, 100, 75, 50, 35, 20, 10 and 5 m with or without idle mode capabilities. The rest of the parameters are  $d = 300$  UE/km<sup>2</sup>,  $ud=1$ ,  $s = 1$ ,  $f = 2$  GHz,  $a = 1$  and  $t = 12$  dB.

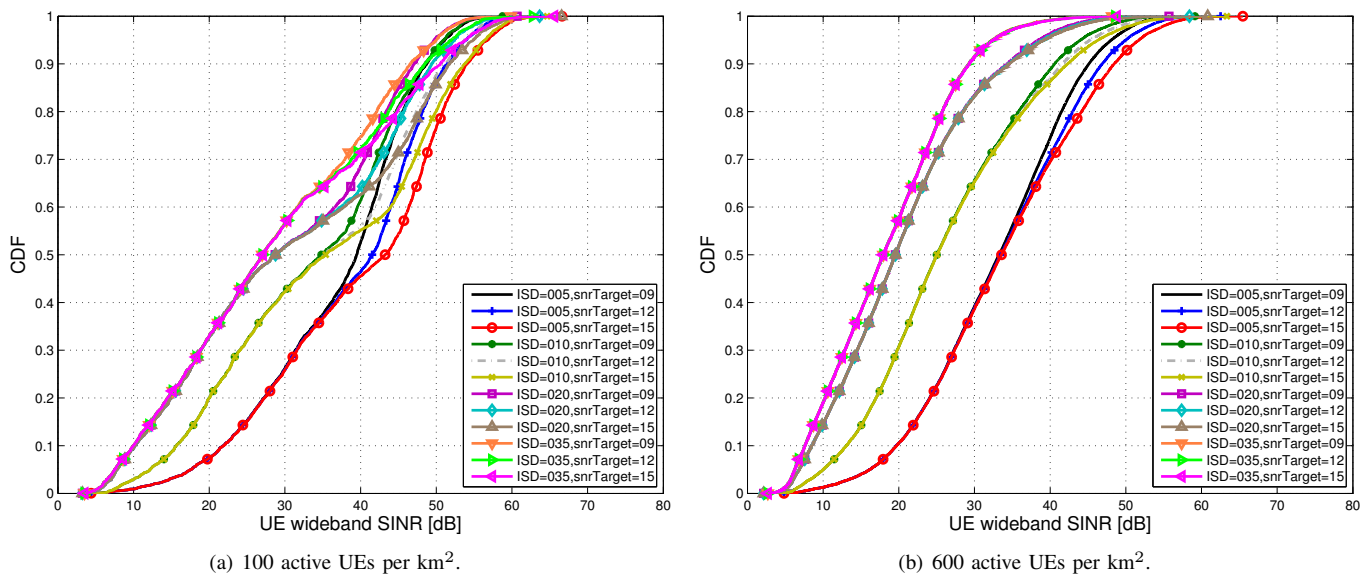


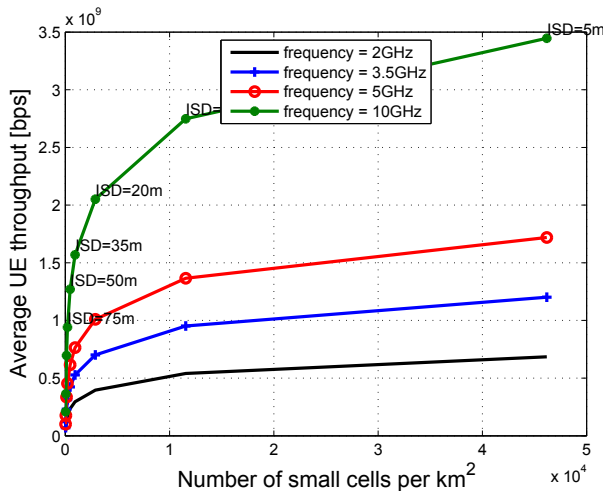
Fig. 11. UE SINR CDF in ultra-dense small cell deployments with large BS densities, 35, 20, 10 and 5 m, low UE densities, 100 and 600 active UEs per km<sup>2</sup> and SNR targets, 15, 12 and 9. The rest of the parameters are  $ud=1$ ,  $s = 1$ ,  $f = 2$  GHz, and  $a = 1$ .

not occur. It is important to note that even in the indicated cases the decoupling of the UE SINR CDF only happens at the high SINR regime, whose SINRs belong to non-cluster UEs suffering from low interference. As a result, since the decoupling only happens for a very extreme BS density, it can be concluded that such transition from interference limited to noise limited does not occur in realistic deployments, and that the small cell BS transmit power should be simply configured to guarantee a targeted range.

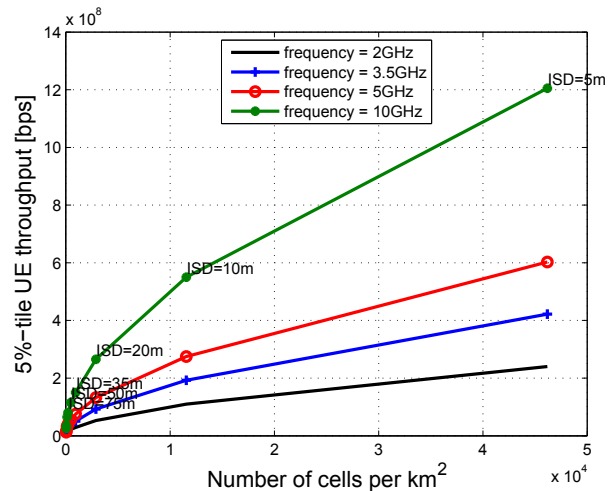
## VI. HIGHER FREQUENCY BANDS

As shown by the Shannon-Hartley theorem presented in (1), network capacity linearly increases with the available

bandwidth. Therefore, increasing the available bandwidth is an appealing proposition to enhance network capacity. However, spectrum is a scarce resource, specially at the lower frequency bands, [500-2600] MHz, which are in use today by radio and TV stations as well as the first wireless communication systems due to their good propagation properties. These frequency bands are thus heavily regulated, and it is unlikely that large bandwidths become available from them in the near future. As a result, in the quest to increase network capacity, vendors and operators have started to look at the usage of higher frequency bands,  $\geq 3500$  MHz, where large bandwidths  $\geq 100$  MHz are available. Due to the higher path losses at higher frequency bands, these bands were never appealing for large macrocells

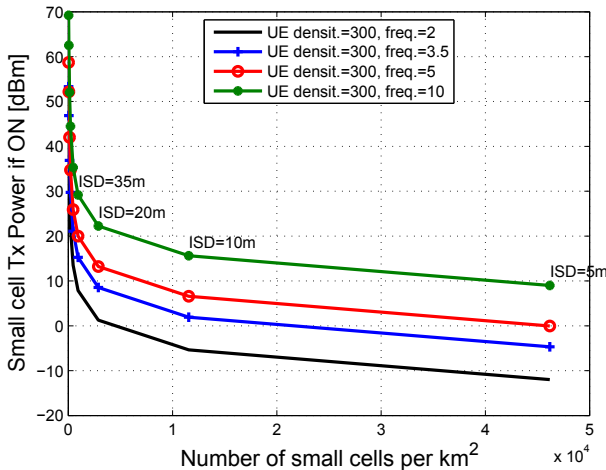


(a) Average UE throughput for different frequency bands.



(b) 5%-tile UE throughput for different frequency bands.

Fig. 12. Average and 5%-tile UE throughput for four different network configurations where the carrier frequencies are 2.0, 3.5, 5.0 or 10 GHz. The rest of the parameters are  $d = 300 \text{ UE/km}^2$ ,  $ud=1$ ,  $s = 1$ ,  $a = 1$  and  $t = 12 \text{ dB}$ .



(a) Transmit power per active BS for different frequency bands.

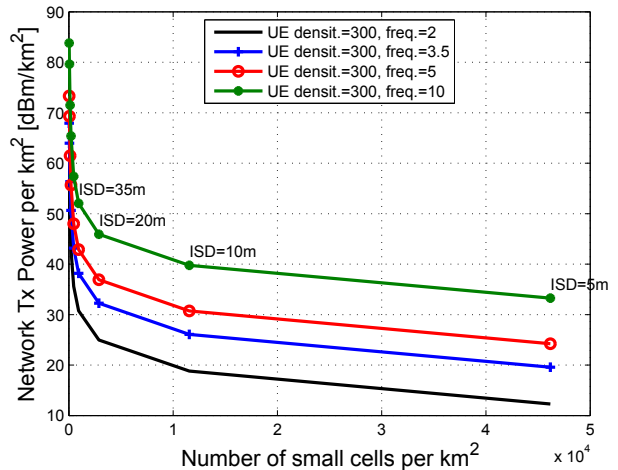
(b) Transmit power of the network per km<sup>2</sup> for different frequency bands.

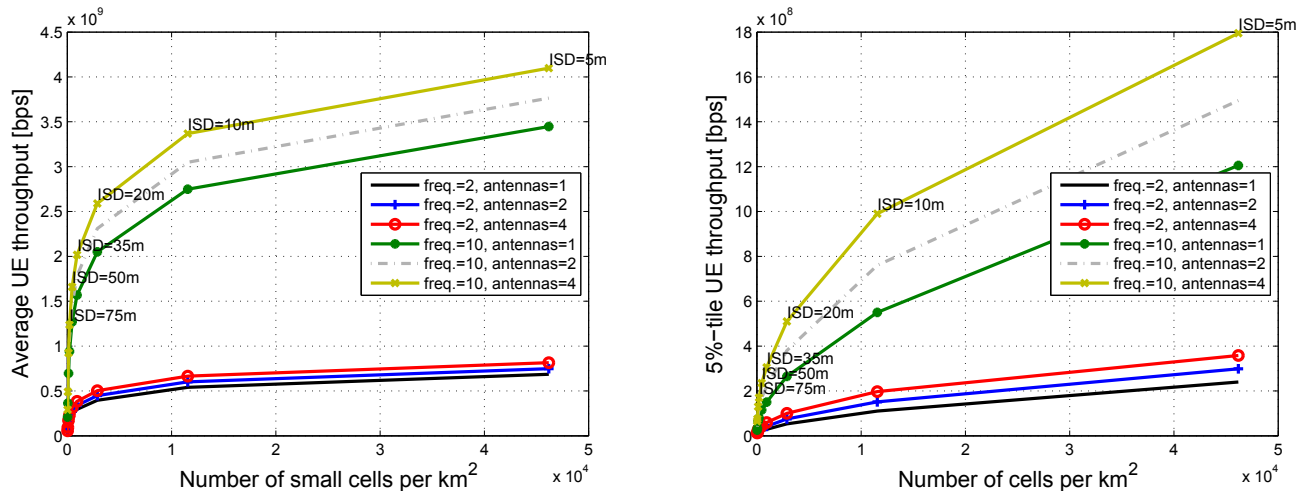
Fig. 13. Transmit power per active BS and transmit power of the network per km<sup>2</sup> for different network configurations where the carrier frequencies are 2.0, 3.5, 5.0 or 10 GHz. The rest of the parameters are  $d = 300 \text{ UE/km}^2$ ,  $ud=1$ ,  $s = 1$ ,  $f = 2 \text{ GHz}$ ,  $a = 1$  and  $t = 12 \text{ dB}$ .

but now suit well the operation of small cells, targeted at short ranges. These higher path losses should not only be considered as a disadvantage but also as an opportunity, since they effectively mitigate interference from neighbouring cells, and thus allow a better spatial reuse. Moreover, it allows using smaller antennas and packing more of them per unit of area, which benefits multi-antenna techniques. In the following, the capacity gains provided by and the challenges faced when using higher frequency bands are discussed.

In order to assess the capacity gains provided by ultra-small cell deployments and the use of higher frequency bands, Fig. 12 shows the average and 5%-tile UE throughput for different densification levels and four different network configurations where the carrier frequencies are 2.0, 3.5, 5.0 and 10 GHz and the available bandwidth is 5% of the carrier frequency, i.e., 100, 175, 250 and 500 MHz, respectively. In

this case, the targeted SNRs by the small cell BSs at  $\frac{\sqrt{3}}{2}$  of the ISD is 12 dB. thus assuring a constant coverage area regardless of the frequency band. From the results, different observations can be made. Based on Fig. 12, in the following we first analyse the impact of densification in network capacity and then improvements brought by the use of higher frequency bands.

In terms of densification, the average and 5%-tile UE throughput do not increase linearly with the number of deployed BSs, but with diminishing gains. This is due to the finite nature of UE density and the characteristic of its distribution. In a first phase, with a low BS density and up to an ISD of 35 m, the UE throughput rapidly grows, almost linearly with the number of cells, due to cell splitting gains and spatial reuse. Subsequently, in a second phase, once the fundamental limit of spatial reuse is reached – *one UE per*



(a) Average UE throughput for different number of antennas per BS and (b) 5 %-tile UE throughput for different number of antennas per BS and frequency bands.

Fig. 14. Average and 5%-tile UE throughput for different network configurations where the carrier frequencies are 2.0 or 10 GHz and the number of antennas per BS are 1, 2 or 4. The rest of the parameters are  $d = 300$  UE/km<sup>2</sup>,  $ud=1$ ,  $s = 1$ ,  $f = 2$  GHz and  $t = 12$  dB.

cell – the UE throughput continues growing at a lower pace with the network densification. This is due to the combined effect of both, bringing the UE closer to the serving cell BS through densification and further from the interfering BSs through idle modes. These two effects together results in a SINR enhancement. These transition and two regimes are more obvious for the average than for the 5 %-tile UE throughput, since cell-edge UEs benefit more from proximity gains and interference mitigation.

Looking at the average and 5 %-tile UE throughput using the 200 m ISD case with a 100 MHz bandwidth as a baseline, the 35 m ISD case can provide an average and cell-edge gain of  $7.56\times$  and  $5.80\times$ , respectively, while the gains provided by the 5 m ISD case are  $17.56\times$  and  $48.00\times$ . This shows that a significant increase in network performance can be achieved through network densification.

In terms of frequency bands, the average and 5 %-tile UE throughput increase linearly with the carrier frequency due to the larger available bandwidth, showing the use of larger bandwidth as a key to achieve larger UE throughputs.

Looking at the average and 5 %-tile UE throughput with the 35 m ISD case with a 100 MHz bandwidth as a baseline, a bandwidth of 250 MHz can provide an average and cell-edge gain of  $2.59\times$  and  $2.58\times$ , while the gains provided by a bandwidth of 500 MHz are  $5.31\times$  and  $5.17\times$ . Although not as large as the gains provided by network densification, they also represent a significant increase in network performance.

It is important to highlight that the capacity gains seen through using higher frequency bands do not come for free. The cost of the UE and BS equipment increases with the carrier frequency, as more sophisticated analogue circuit components are needed. Moreover, a larger transmit power is required for both lighting up the more subcarriers existing in a wider bandwidth and compensating for the higher path losses at higher frequency bands [68]. Fig 13 shows how both the transmit power per active BS and the overall transmit power

used by the network increases with the wider bandwidth and the larger path losses, where this increase is not negligible and up to 24.34 dB. This transmit power increase is prohibitive in macrocell BSs where the required power would be up to 70 dBm, but it is still well suited to ultra-dense small cell deployments where BSs could operate this large bandwidth with less than 20 dBm of transmit power. In order to reduce transmit power, the identification and characterisation of hot spots becomes critical [69] [70] since deploying BSs where they are most needed, e.g., right in the middle of a circular hot spot, will decrease the average UE path loss to the serving BS, and reduce this transmit power. Lighting up only those subcarriers with good channel quality that are necessary to achieve the required UEs throughput targets will also help to reduce transmit power.

From the results, one can see that, when combining network densification with increased bandwidth, the targeted average 1 Gbps per UE is reachable with an ISD of 50m and 500 MHz bandwidth, or 20 m ISD and 250 MHz bandwidth. The first and the second combination resulting in an average of 1.27 Gbps and 1.01 Gbps per UE, respectively. Thus, it can be concluded that the usage of larger cellular bandwidth than today's 100 MHz is required to meet the expected high data rates.

Taking the usage of higher frequency bands to an extreme, vendors and operators have also started to look at exploiting mmWave with carrier frequencies on 22, 60 and 77 GHz, where the available bandwidth is enormous,  $\geq 1$  GHz [71]. However, diffraction and penetration through obstacles are hardly possible at these high frequency bands, and thus only LOS or near-LOS links seem feasible. In addition, the range of the cell may be confined by high atmospheric phenomenas. Water and oxygen absorption significantly increase path losses, especially at 22 GHz and 60 GHz, respectively. As a result, providing the required coverage range through larger transmit powers is not feasible anymore, as it is in the sub-10 GHz bands. Thus, it is expected that active antenna arrays and

beamforming techniques become essential to overcome the increased path losses at these high frequency bands [52].

## VII. MULTI-ANTENNA TECHNIQUES AND BEAMFORMING

Previous results showed that for a single antenna small cell BS, the targeted average 1 Gbps per UE is only reachable with an ISD of at least 50 m and a bandwidth of 500 MHz (or 35 m and a bandwidth of 250 MHz). In order to enhance UE performance and bring down this still large BS density, the usage of multiple antennas at the small cell BS is explored in the following.

Multiple antenna systems provide a number of degrees of freedom for transmitting information, which may vary from one to a number upper bounded by the number of antennas. The higher the number of degrees of freedom available, the better spectral efficiency can be expected. However, how many effective degrees of freedom are available is mostly related to the spatial correlation of the channels [72]. Given a number of degrees of freedom available, two multi-antenna techniques stand out. Beamforming makes use of only one of the degrees of freedom available, while spatial multiplexing may use all of them. Beamforming benefits from a low complexity implementation, together with its ability to extend the cell range by focusing the transmit power in a certain direction. However, it may be suboptimal in terms of spectral efficiency. In contrast, spatial multiplexing has the potential to approach the maximum channel capacity, linearly increasing the capacity of the channel with the minimum of number of transmit and receive antennas. However, it is significantly more complex to implement [72].

This paper focuses on quantised maximal ratio transmission (MRT) beamforming, using the standardised LTE code book beamforming approach [73], partly due to its simplicity and partly due to the fact that the small cell sizes in an ultra-dense deployment may result in a large spatial correlation of the channels, thus limiting the degrees of freedom available and rendering spatial multiplexing unsuitable. The effectiveness of spatial multiplexing in ultra-dense small cell deployments is left for future analysis.

Here, it is assumed that each BS is equipped with a horizontal antenna array comprised of 1, 2, or 4 antenna elements, and each UE has a single antenna. The existing transmit power is equally distributed among antennas. The characteristics of the antenna elements used in this analysis are described in Appendix A. Based on measurements over BS pilots signals, the UE suggests to the BS the precoding weights specified in the LTE code book [74] that maximise its received signal strength, and the BS follows such suggestion. This horizontal beamforming helps to shape the horizontal antenna pattern at the BS and thus focus the energy towards the UE in the horizontal plane. Interference mitigation is also achieved in an opportunistic manner [75]. Real-time inter-BS coordination required for cooperation is not supported.

Fig. 14 shows the average and 5%-tile UE throughput for different network configurations where the carrier frequencies are 2.0, 3.5, 5.0 and 10 GHz and the number of antennas per BS are 1, 2 or 4. Control channels are not beamformed.

The targeted SNRs by the small cell BS at  $\frac{\sqrt{3}}{2}$  of the ISD is 12 dB. thus assuring a constant coverage area regardless of the frequency band. The constant coverage is maintained at the expense of larger transmit power, as explained earlier. Different remarks can be made based on the results.

Beamforming gains increase in a diminishing manner with the number of antennas. This is in line with the linear antenna array theory, which indicates that beamforming antenna gains increase logarithmically with the number of antennas [76]. Looking at the average UE throughput for the 35 m ISD case with a 500 MHz bandwidth, the average gain of using 2 antennas over 1 antenna is 13.77 % (1 more antenna is needed), while the gain of using 4 antennas over 2 antenna is 13.05 % (2 more antennas are needed). The overall average gain from 1 to 4 antennas is 18.92 %.

Beamforming gains are larger at the cell-edge. This is because of the interference mitigation provided by the beamforming, which is more noticeable at the cell-edge. Looking at the cell-edge UE throughput for the 35 m ISD case with a 500 MHz bandwidth, the cell-edge gain of using 2 antennas over 1 antenna is 46.67 % (1 antenna increase), while the gain of using 4 antennas over 2 antennas is 38.63 % (2 antennas increase). The overall cell-edge gain from 1 to 4 antennas is 48.96 %.

Beamforming gains are larger for larger cell sizes. This is because the beamforming helps improving the received signal strength of UEs, which may receive only a poor received signal strength if beamforming is not in place. For the 200 m ISD and the 5 m ISD cases with a 500 MHz bandwidth, the average gains of using 2 antennas over 1 antenna are 19.05 % and 9.23 %, respectively (1 antenna increase), while the gains of using 4 antennas over 2 antenna are 17.37 % and 8.87 %, respectively (2 antennas increase).

From the results, one can see that the targeted average 1 Gbps per UE is now reachable with an ISD of 75 m, 500 MHz bandwidth and 4 antennas (or 35 m, 250 MHz bandwidth and 4 antennas), showing that multi-antenna techniques enhance UE performance and can bring down BS density to meet the targeted UE demands. However, overall, beamforming gains are estimated to be of the order of up to 1.49x, which are poor compared to the larger gains provided by network densification and use of higher frequency bands. Therefore, since the larger path loss at the frequency bands between 2 and 10 GHz could be compensated via larger transmit powers, the existing antennas at the small cell may be better exploited by using spatial multiplexing, which has the potential to linearly increase the performance with the number of antennas provided that the required degrees of freedom exists in the channel. Spatial multiplexing in ultra-dense small cell networks is one of our future lines of research.

## VIII. SCHEDULING

In LTE, a Resource Block (RB) refers to the basic time/frequency scheduling resource unit to which a UE can be allocated. Each RB expands 180 KHz in the frequency domain and has a duration of 1 ms in the time domain. The RB consists of 12 subcarriers of 15 KHz and its 1 ms Transmission Time Interval (TTI) is referred to as a subframe.

Unlike other diversity techniques that aim to average the signal variations to mitigate the destructive impact of multi-path fast fading, channel dependent scheduling takes advantage of multi-path fading by allocating to each RB the UE having the best channel conditions. This is one of the main enhancements of LTE over Universal Mobile Telecommunication System (UMTS) [77]. Such type of scheduling leads to multi-user diversity gains, which have been shown to roughly follow a double logarithm scaling law in terms of capacity with regard to the number of UEs per BS in macrocell scenarios [78]. It is important to note that in order to aid the channel sensitive scheduling and exploit multi-user diversity gains, UEs need to report DL Channel Quality Indicator (CQI) back to their serving BSs, which allows the scheduler to assess the UE channel quality and perform the scheduling according to a specified metric.

In a network with  $U$  UEs, each UE may undergo varying channel conditions where better channel quality generally refers to higher signal quality and higher throughput. Sharing the resources fairly between UEs experiencing different channel qualities is a challenging task [79]. In the following, a survey of traditional small cell schedulers is provided.

*Opportunistic* schedulers select the UE with the best channel quality at each time/frequency resource, aiming to solely maximise the overall throughput, whereas *Round Robin (RR)* schedulers treat the UEs equally regardless of their channel quality, giving them the same share of time/frequency resources. The former scheduler can increase system throughput remarkably compared to the latter at the expense of fairness, since UEs with relatively bad channel qualities may be never scheduled [80]. *Proportional Fair (PF) schedulers*, in contrast, exploit multi-user diversity based on UE CQIs, attempting to maximise the throughput while simultaneously reinforcing a degree of fairness in serving all the UEs.

The PF scheduling metric basically aims at weighting the UE's potential instantaneous performance by its average performance, and PF schedulers usually consists of three stages. In the first stage, according to buffer information, the schedulable set of UEs is specified. The second stage is the time domain scheduling, which is in charge of reinforce fairness and selects the  $N_{max}$  UEs that will be input to the frequency domain scheduler, and thus be allocated RBs in the current subframe. The last stage corresponds to the frequency domain scheduling, i.e., allocation of UEs to RBs. The complexity of the frequency domain scheduler highly depends on the number of its input UEs [81] [82], and thus the time domain scheduler has a major impact on the complexity of the frequency domain scheduler.

Multiple time domain and frequency domain PF metrics exist [81]. A PF scheduling metric in time domain can be defined as

$$M_{m,u}^{\text{PF-TD}} = \frac{\hat{D}_{m,u}}{R_{m,u}}, \quad (2)$$

where  $R_u$  and  $\hat{D}_u$  are the past average throughput and potential instantaneous throughput of the  $u^{\text{th}}$  UE connected to the  $m^{\text{th}}$  BS, respectively [81], and the past average throughput is calculated using a moving average. The UEs will be

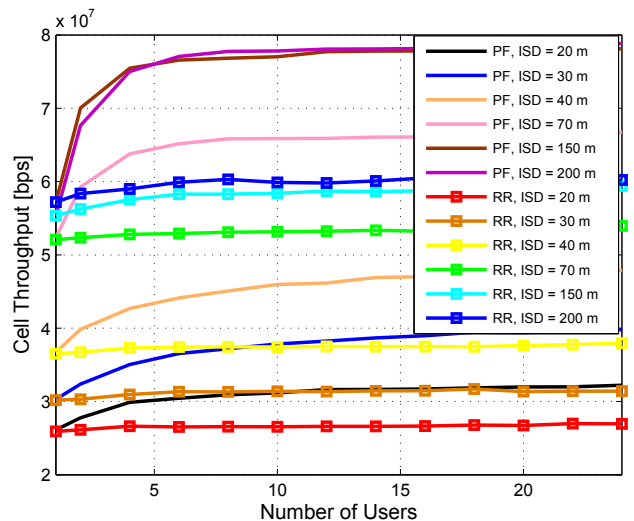


Fig. 15. Average cell throughput for various ISD with RR and PF schedulers.

then ranked constantly according to the metric in (2), and the  $U_{max}$  UEs with maximum preference are passed on to the frequency domain scheduler. A PF scheduling metric in frequency domain can be defined as

$$M_{m,u,k}^{\text{PF-FD}} = \frac{\gamma_{m,u,k}}{\sum_{k=1}^{N_{RB}} \gamma_{m,u,k}}, \quad (3)$$

where the numerator  $\gamma_{u,k}$  is the SINR of the  $u^{\text{th}}$  UE connected to the  $m^{\text{th}}$  BS on the  $k^{\text{th}}$  RB and the denominator is the sum of the  $u^{\text{th}}$  UE SINRs over all RBs, which represents its average channel quality at specified subframe [81]. The UEs will be ranked constantly according to the metric in (3), and the UE with maximum preference is selected to be served on the  $k^{\text{th}}$  RB.

It is important to note that channel gain fluctuations occur from RB to RB due to multi-path fast fading. In order to consider the multi-path fast fading effect in this section, the BS to UE channel gain  $G_{m,u}$  [dB] also comprises the multi-path fast fading gain, which is modelled using a distant dependent Rician channel. The lower the UE to serving BS distance, the lower the channel fluctuations due to multi-path fading [63]. This model is presented in Appendix A.

In the following, the performance of RR and PF schedulers is analysed under different densification levels.

Fig. 15 shows the performances of RR and PF schedulers in terms of cell throughput with respect to the number of served UEs per BS for different ISDs. Let us look first at the trends. When using RR, the number of served UEs per BS does not impact the cell throughput, since RR does not take into account the UE channel quality and therefore does not take advantage of multi-user diversity. In contrast, PF is able to benefit from multi-user diversity, and the cell throughput increases with the number of served UEs per BS up to a given extent. There is a point in which having more UE per BS does not bring any cell throughput gains, and this point is lower with the network density. For this particular case, having more than

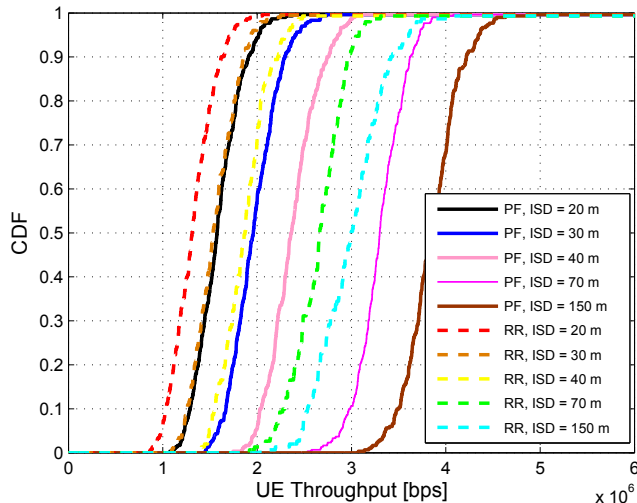


Fig. 16. CDF of UE throughput for different ISDs.

8 UEs per cell does not noticeably increase cell throughput for an ISD of 200m, while this number is reduced to 6 UEs for an ISD of 20m. Multi-user diversity gains vanishes with network densification due to stronger LOS propagation and less fluctuating channel conditions. Paying now attention to the overall per cell performance, although PF always outperforms RR, it is important to note that the PF scheduler starts losing its advantage with respect to RR in terms of cell throughput with the reduced cell size. For a given number of UE per BS, let's say 4, the PF gain over RR reduces from 21.2% to 12.4% and 10.5% for ISDs of 150, 40 and 20m, respectively.

Shrinking the cell size not only reduces cell throughput but also reduces UE throughput. Applying the PF scheduler, Fig. 16 shows that due to both interference enhancement due to NLOS to LOS transition as well as multi-user diversity loss due to low channel fluctuations, the UE throughput for a given number of served UEs per BS drops down with network densification. For instance, reducing the ISD from 150m to 40m and 20m, the UE 5%-tile throughput drops by  $\sim 40.8\%$  and  $\sim 36.7\%$ , respectively. Comparing the UE 5%-tile throughput of PF and RR for an ISD of 20m, the gain of the former is almost negligible, around  $\sim 9\%$ .

The minor gains of PF scheduler over the RR one at low ISDs in terms of cell and UE throughput suggests that RR scheduler may be a better choice in dense small cell deployments considering its lower complexity. The complexity of PF lies in the evaluation of each UE on each RB considering a greedy PF that operates on a per RB. The PF complexity with exhaustive search is considerably higher. This conclusion may have a significant impact in the manufacturing of small cell BSs where the Digital Signal Processor (DSP) cycles saved due to the adoption of RR scheduling can be used to enhance the performance of other embedded technologies.

## IX. ENERGY-EFFICIENCY

Deploying a large number of small cells, millions, tens of millions, poses some concerns in terms of energy consump-

tion. For example, the deployment of 50 million femtocells consuming 12 Watts each will lead to an energy consumption of 5.2 TWh/a, which is equivalent to half the power produced by a nuclear plant [83]. This approach does not scale, and thus the energy efficiency of ultra-dense small cell deployments should be carefully considered to allow the deployment of sustainable networks.

In Section V, Fig. 8(b) showed how the overall transmit power used by the network significantly reduces with the small cell BS density when an efficient idle mode capability is used. This is because the reduction of transmit power per cell outweighs the increased number of active cells. However, this observation may not hold when considering the total power consumption of each small cell BS, since a BS in idle mode may still not consume a non-negligible amount of energy, thus impacting the energy efficiency of the network. In order to better understand the impact of network densification on the power consumption, the energy efficiency of ultra-dense small cell networks in terms of throughput per Watt ([bps/W]) is analysed in the following.

This study uses the power model developed by the GreenTouch project [84]. This power model estimates the power consumption of a cellular BS, and is based on tailored modelling principles and scaling rules for each BS component i.e., power amplifier, analog front-end, digital base band, digital control and backhaul interface and power supply. Moreover, it provides a large flexibility: multiple BS types are available, they can be configured with multiple parameters (bandwidth, transmit power, number of antenna chains, system load, etc.) and include different optimised idle modes. Among the provided idle modes, we considered the GreenTouch slow idle mode and the GreenTouch shut-down state, where most or all components of the BS are deactivated, respectively. These two modes are the most efficient ones provided by the model.

Table II shows the estimated power consumption for different small cell BS types with different transmit power, where such power consumption is given for the active mode (full load) as well as the slow idle mode and the shut-down state, and for BSs with 1, 2 or 4 antennas. Note that we used the 2020 small cell BS type in the model and that the presented analysis considers a 20 MHz bandwidth. In contrast to macrocell BSs, it is important to realise that the power consumption of a small cell BS linearly scales with the number of antenna chains, since it is the most contributing component to power consumption in a small cell BS.

Based on the values of Table II and the throughput analysis in previous sections, Fig. 17 shows the energy efficiency in bps/W for different network configurations with 1, 2 or 4 antennas per BS. The idle mode profile is indicated by  $sm$ . In addition to the slow idle mode ( $sm=1$ ) and the shut-down state ( $sm=2$ ) models provided by the GreenTouch project, three futuristic idle modes are considered, where their energy consumption is 30% ( $sm=3$ ), 15% ( $sm=4$ ), or 0% ( $sm=5$  - idle small cell does not consume anything) of the GreenTouch slow idle mode power consumption model ( $sm=1$ ).

For any given idle mode, results show that increasing the number of antennas at the small cell BS always decreases the energy efficiency. This is because the performance gain

provided by adding a new antenna through beamforming is not large enough to cope with the increase in power consumption resulting from adding a new antenna chain at the small cell BS. A different conclusion may be obtained for the macrocell case, where adding a new antenna chain does not lead to a large increase in the total power consumption of the BS, since other components consume much more energy. Conclusions for the small cell BS case may be different when considering spatial multiplexing instead of beamforming. Indeed, provided that the required degrees of freedom exists in the channel, the performance of spatial multiplexing in terms of capacity can follow a linear scaling law with the minimum number of transmit and receive antennas, and this capacity boost will enhance energy efficiency.

When comparing the performance of the different idle modes in terms of energy efficiency, it can be seen that the lower the power consumption in the idle mode, the larger the energy efficiency of the network. This is because less energy is required to transmit the same amount of bits at the network level. When using the idle mode models provided by the GreenTouch project, idle modes 1 and 2, energy efficiency decreases with densification. This is because the increase in throughput provided by adding more cells is not large enough compared to the increase in their power consumption, mostly because idle cells following the GreenTouch project model still consume a non-negligible amount of energy. When considering the energy consumption of the futuristic idle modes 3 and 4, this trend starts changing. First, the energy efficiency increases with densification, and then starts decreasing when the number of deployed cells becomes large and many cells are empty. It is important to notice that when considering the energy consumption of the new idle mode 5, idle cells do not consume anything, the trend significantly changes. Energy efficiency always increases with densification, and it does it in a significant manner. This is because the increase in throughput provided by adding more cells comes now at a no or very low energy cost since idle cells do not consume power from the energy grid.

This last observation shows the need for the development of more advanced idle mode capabilities, where the power consumption of a small cell BS from the energy grid in idle mode is zero. This can be optimally realised by using energy harvesting approaches that are able to supply sufficient power to keep the small cell BS alive when it is in idle mode. For example, assuming the use of idle mode 2 and 4 antennas at the small cell BS, the energy harvesting mechanism would need to provide the affordable amount of 0.4073 W to make ultra-dense small cell deployments energy efficient. In this area, researchers are looking at both thermoelectric as well as mechanical energy harvesting techniques. An example of the latter is the research in [85] and [86], based on vibration energy harvesting techniques for powering wireless sensors and small cell infrastructure. Moreover, an issue with all ambient environment energy sources, to varying degrees, is their intermittent nature. For example, harvesting useable levels of solar and wind power is dependent on the time of the day, the season and the local weather conditions. For this reason, an efficient and cost-effective energy storage

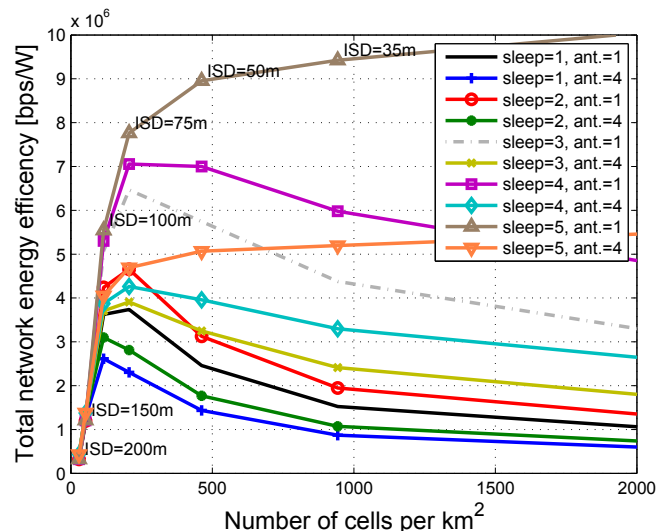


Fig. 17. Energy efficiency in bps per Watt for different network configurations where the carrier frequency is 2.0GHz, the bandwidth is 20MHz, and the number of antennas per BS are 1, 2 or 4. The rest of the parameters are  $d = 300$  UE/km<sup>2</sup>,  $ud=1$ ,  $s = 1$ ,  $f = 2$  GHz and  $t = 12$  dB.

system is also key [87]. These are important areas of research, whose results are vital to deploy energy efficient and green telecommunications networks that have a minimal impact in the ecosystem.

## X. WHAT IS DIFFERENT IN ULTRA-DENSE SMALL CELL DEPLOYMENTS

In this section, the main differences between regular HetNets and ultra-dense HetNets are highlighted.

**Difference 1 - BS to UE density:** UE density is larger than BS density in regular HetNets, while UE density is smaller than BS density in ultra-dense HetNets. BSs with no active UEs should be powered off to reduce unnecessary interference and to conserve power in ultra-dense HetNets, which is considered in the numerical/analytical results for regular HetNets.

**Difference 2 - Propagation conditions:** NLoS interferers count for most cases in regular HetNets, while LoS interferers count for most cases in ultra-dense HetNets. More sophisticated and practical path loss models should be considered for ultra-dense HetNets, while the simple single-slope path loss model is usually assumed to obtain the numerical/analytical results for regular HetNets.

**Difference 3- Diversity loss:** Rich UE diversity in regular HetNets, while limited UE diversity in ultra-dense HetNets. Independent shadowing and multi-path fading among UEs in one cell is usually assumed in regular HetNets to obtain the numerical/analytical results. Such assumption is not true in the ultra-dense HetNets. Thus, new results for the ultra-dense HetNets should be derived.

As a result of these differences, the numerical/analytical results for regular HetNets cannot be directly applied to ultra-dense HetNets due to different assumptions for the fundamental characteristics of the networks.



TABLE II  
POWER CONSUMPTION.

Small cell ISD (m)	Tx Power (dBm/mW)	Consumed Power (W)								
		Full load			idle mode 1 ( $sm=1$ )			idle mode 2 ( $sm=2$ )		
		1 antenna	2 antenna	4 antenna	1 antenna	2 antenna	4 antenna	1 antenna	2 antenna	4 antenna
200	23.27/212.32	1.8923	2.5848	4.4560	0.2324	0.3105	0.4959	0.1881	0.2478	0.4073
150	20.52/112.72	1.3405	2.0316	3.9015	0.2191	0.2971	0.4825	0.1748	0.2345	0.3939
100	16.64/46.13	0.9793	1.6696	3.5386	0.2104	0.2884	0.4738	0.1661	0.2257	0.3852
75	13.90/24.55	0.8643	1.5544	3.4231	0.2076	0.2856	0.4710	0.1633	0.2230	0.3824
50	10.02/10.05	0.7853	1.4752	3.3437	0.2057	0.2837	0.4691	0.1614	0.2210	0.3804
35	6.61/4.58	0.7558	1.4456	3.3141	0.2050	0.2830	0.4683	0.1607	0.2203	0.3797
20	1.27/1.34	0.7383	1.4281	3.2965	0.2046	0.2826	0.4679	0.1603	0.2199	0.3793
10	-5.20/0.30	0.7326	1.4224	3.2908	0.2044	0.2824	0.4678	0.1601	0.2198	0.3792
5	-11.89/0.06	0.7314	1.4211	3.2895	0.2044	0.2824	0.4678	0.1601	0.2197	0.3791

## XI. CHALLENGES IN ULTRA-DENSE SMALL CELL DEPLOYMENTS

In this section, the main challenges faced on the way to ultra-dense small cell deployments are highlighted.

### Challenge 1 - Backhaul:

Recent surveys show that 96% of the operators consider backhaul as one of the most important challenges to small cell deployments, and this issue is exacerbated in ultra-dense ones [88] [89]. While today's wireless backhaul solutions may be a choice in higher network tiers, we anticipate that they will only be a solution up to a certain extent in ultra-dense small cell deployments. Due to the high capacity requirements, wired backhaul will likely be a key requirement for these deployments, and thus this type of network only makes sense in dense urban scenarios, where the traffic demands are the highest and the city infrastructure can provide dense fibre and/or Digital Subscriber Line (DSL) connectivity to operators. The existing backhaul capability may well influence the deployment of the small cell BSs. Massive MIMO multicast is also a promising solution to provide backhaul to a large number of underlaid small cells [52]. However, this technology still faces its own challenges, architecture and hardware impairments [90], pilot contamination [91] and accurate CSI acquisition [92] may be still an issue to provide a global solution. Other wireless backhaul technologies include two-way relaying [93], or even four-way relaying [94]. However, as explained earlier, such solution might not be scalable to ultra-dense small cell networks. Hence, their usage is envisaged to be limited in practice.

### Challenge 2 - Mobility:

As indicated in Section II, we anticipate a future network architecture comprised of different small cell tiers with different types of small cell BSs, targeted at different types of environments and traffic, where dedicated channel mid-frequency small cell deployments with the macrocell tier may be ultra-dense to enhance network capacity. Within this architecture, mobile UEs should be kept in the macrocell tier, while static UEs should be handed over to the ultra-dense small cell tier. In order to realise this, a new mobility management approach is needed, in which UEs only take measurements and access the cells of the appropriate network tier according to their velocity. Accurate mobility state estimation is key to realise this [95]. Splitting the transmission of the UE control and data planes will also provide mobility robustness, allowing the larger cells to transmit and manage control/mobility related information, while the smaller cells provide the majority of the data traffic [40]. However, this new architecture poses

challenges in the management of data bearers towards the core network, since in order to realise the mobility benefits, the data bearer should be anchored at the cell in the higher network tier (e.g. macrocells), and this one forward the information to the cell in the lower network tier (e.g. small cells) [96]. If many small cells anchor to the same macrocell, the latter may become a bottleneck.

### Challenge 3 - Reducing costs:

In order to improve the cost efficiency of network deployments, it is important that small cell BS are developed in enormous numbers to take advantage of an economy of scale. Moreover, CAPEX and OPEX should be brought to a minimum. In order to reduce CAPEX, the price of small cell BS should be considered, which may require the use of cheap filters, power amplifiers and other components. Small cell BSs may also be deployed by the end users themselves to leverage existing power and back-haul infrastructure, thus reducing OPEX [97]. Moreover, in order to deploy a larger number of cells cost effectively in a short period of time, it is required that the cells can be deployed in a plug & play manner and do not require any human involvement for optimisation. Self-organisation capabilities are thus key to manage an ultra-dense small cell deployment. For example, the approach in [98] ensures that the small cell coverage is confined within the targeted household through power control and antenna switching techniques, thus minimising necessary handovers. The approach in [99] maximises capacity by using machine learning techniques at the small cell to learn where the UEs are clustered and beamforming to point its antenna beam towards such hotspot. Neighbouring cell list optimisation is also a key issue in ultra-dense small cell networks where neighbouring cells are switched on and off in a dynamic manner [100].

### Challenge 4 - Small cell location planning:

Finding hotspots and characterising their traffic is of crucial importance in order to deploy the right number of small cells in the right positions according to UE needs. Misunderstanding this information can result in an under- or over-estimated number of deployed cells, which will affect both energy and cost efficiency as well as network performance. However, finding and characterising hot spots is not an easy task since UE traffic is not usually geolocated, and network operators mostly rely today on inaccurate proximity or triangulation approaches. Fingerprinting approaches are a possible solution to enhance the accuracy of geolocation [101].

### Challenge 5 - Smart idle mode capabilities:

As shown in the paper, the availability of an efficient idle mode capability at the small cell BSs is key in order to mitigate inter-cell interference and save energy. In idle mode, it is important that small cell BSs minimise signalling transmissions and consume as little power as possible. Indeed, our previous results show that in order to achieve energy efficient deployments, a small cell BS in idle mode should not consume any power. To realise this, aside from the LTE solution based on DRSs [39] (see Section III-B), another feasible solution would be to equip the small cell BS with a sniffing capability, as proposed in [62], such that the small cell BSs is idle and switches off most of the small cell BS modules when it is not serving active UEs. When the small cell is idle, it transmits no signalling, and wakes up upon the detection of uplink signalling from the UE towards the macrocell tier. However, this solution does not allow selective wake-ups, where only the most adequate cell in a cluster of idle cells wakes up to serve the incoming UE. Moreover, it is important to note that smart idle mode capabilities imply UE-oriented operations, and thus should be performed in a dynamic manner, considering the traffic dynamics of large variety of UEs. Dynamic small cell idle mode control also poses new challenges such as the ping-pong cell re-selection. To be more specific, a suddenly powered-on BS might confuse idle UEs since they need to re-select cells according to the best-Reference Signal Received Power (RSRP) rule, and then go back to their previous cells when the small cell BS returns to idle mode. The ping-pong cell re-selection greatly consumes UEs battery life and it should be avoided.

#### **Challenge 6 - Modulation and coding schemes:**

Deploying higher order modulation and coding schemes is critical to take advantage of the high SINRs resulting from ultra-dense small cell deployments. Even higher modulation schemes than currently used in LTE and Wireless Fidelity (WiFi), i.e., 256-QAM, may be required, e.g., 1024-QAM. However, this brings about the need for accurate channel state information for coherent de-modulation. However, the implementation feasibility of 1024 or higher QAMs is still unclear due to the Error Vector Magnitude (EVM) issues at transmitters [102]. In addition, the Peak-to-Average Power Ratio (PAPR) problem should also be re-considered for 1024 or higher QAMs.

#### **Challenge 7 - Radio resource management:**

In terms of radio resource management, current scheduling and other network procedures have to be revisited since due to the lower number of UEs per cell, the current approaches used in macrocell may not be optimum anymore. For example, proportional fair scheduling may not be the best solution for very small cells, since there are not many UEs to be fairly served and channel fluctuation may be low due to LOS channel conditions. Simpler solutions may be more appealing such as round robin.

#### **Challenge 8 - Spatial multiplexing:**

Using spatial multiplexing techniques, multiple stream of data can be transmitted simultaneously and successfully decoded at the receiver, provided that the channels corresponding to every pair of transmit and receive antennas are independent. However, the small cell sizes in an ultra-dense small cell

deployment may result in a large spatial correlation of the channels, thus limiting the degrees of freedom available and rendering spatial multiplexing less useful. Therefore, further research is needed in order to understand which is the optimum number of antennas per small cell BSs according to the small cell density, so that beamforming and spatial multiplexing can be exploited in a cost effective manner. Multiuser MIMO is another avenue that should be explored in order to benefit from spatial multiplexing, which as a byproduct may bring down BS power consumption.

#### **Challenge 9 - Dynamic TDD transmissions:**

It can be envisaged that in future networks, small cells will prioritise TDD schemes over Frequency Division Duplexing (FDD) ones since TDD transmissions are particularly suitable for hot spot scenarios with traffic fluctuations in both link directions [103]. In this line, a new technology has recently emerged, referred to as dynamic TDD, in which TDD DL and UL subframes can be dynamically configured in small cells to adapt their communication service to the fast variation of DL/UL traffic demands in either direction. The application of dynamic TDD in homogeneous small cell networks has been investigated in recent works with positive results [18] [19] [104]. Gains in terms of UE packet throughput and energy saving have been observed, mostly in low-to-medium traffic load conditions. However, up to now, it is still unclear whether it is feasible to introduce the dynamic TDD transmissions into HetNets because it will complicate the existing CRE and ABS operations and its advantage in the presence of macrocells in terms of UE packet throughput is currently being investigated [20] [103]. Some pioneering work on the application of dynamic TDD in small cell HetNets can be found in [20].

#### **Challenge 10 - Co-existence with WiFi:**

In order to gain access to more frequency resources, LTE small cells may be deployed in unlicensed bands, where they are required to coexist with WiFi networks. However, when LTE and WiFi nodes are deployed in the same frequency band, WiFi nodes may tend to stay in listening mode waiting for a channel access opportunity, due to their courteous Carrier Sense Multiple Access (CSMA)/Collision Avoidance (CA) protocol and the high-power interference from the LTE network. Simulation results have shown that when co-existing with LTE nodes, if these ones do not implement any co-existence mechanism, WiFi nodes in some indoor scenarios may spend even up to 96% of the time in listening mode due to inter-radio access technology interference and the poor performance of CSMA/CA mechanisms. This significantly degrades WiFi performance [105]. New co-existence solutions have to be devised to enhance LTE and WiFi coexistence and ensure that those two networks share the unlicensed bands in a fair manner. Moreover, it is desirable that the coexistence scheme should be as much frequency agnostic as possible so that a global solution can be achieved. In the 3GPP, a prevailing view is that in the near future, we should first consider unlicensed operation in 5 GHz and focus on DL-only operations assisted by licensed carriers, the so called Licensed Assisted Access (LAA) [14] [106].

## XII. CONCLUSION

In this paper, the gains and limitations of network densification, use of higher frequency bands and multi-antenna techniques have been analysed. Network densification has been shown to provide the most of UE throughput gains of up to 48x at the cell-edge, followed by a linear scale up with the available bandwidth of up to 5x, provided by the use of higher frequency bands. Beamforming gains of around 1.49 at cell-edge have been shown to be low compared to network densification and use of higher frequency bands, and thus the use of spatial multiplexing seems more appealing to exploit the multiple antennas in a BS at the studied frequency carriers, provided that sufficient channel decorrelation among antennas exists.

Efficient idle mode capabilities at the small cells has been shown to be key to mitigate interference and save energy. Moreover, one UE per cell has been shown to be the fundamental limit of spatial reuse and may drive the cost-effectiveness of ultra-dense small cell deployments. As a result, UE density and distribution have to be well understood before any roll-out.

Network densification has also been shown to reduce multi-user diversity, and thus PF alike schedulers lose their advantages with respect to RR ones. For an ISD of 20m, the difference in average UE throughput of PF over RR is only of around 5%, indicating that RR may be more suitable for ultra-dense small cell deployments due to their reduced complexity.

As a bottom line, simulation results have shown that for a realistic non-uniformly distributed UE density of 300 active UE per square km, it is possible to achieve an average 1 Gbps per UE with roughly an ISD of 35m, 250MHz bandwidth and 4 antennas per small cell BS. Today, these deployments are neither cost-effective nor energy efficient. However, this may change in the future with new deployment models, lower cost and more efficient equipment. The top ten challenges to realise cost-effective ultra-dense small cell deployments have also been discussed in this paper.

## APPENDIX

The simulated environment and its channel gains are calculated in form of matrices, representing a two dimensional gain (loss) map with a given resolution [107]. The overall gain is calculated as a sum of individual gains (losses) in decibels for each BS  $m$  and each location as

$$G_m[\text{dB}] = G_{A,m}[\text{dB}] + G_{P,m}[\text{dB}] + G_{S,m}[\text{dB}], \quad (4)$$

where  $G_{A,m}[\text{dB}]$  is the antenna gain,  $G_{P,m}[\text{dB}]$  is the path gain (loss) and  $G_{S,m}[\text{dB}]$  is the shadow fading gain (loss).

The antenna gain  $G_{A,m}[\text{dB}]$  represents the gain resulting from focussing the antenna beam towards one direction. In this case, a vertical half-wave dipole array with four elements spaced by  $0.6\lambda_c$  is used (see Fig. 18 (a)), where the combined gain of the horizontal and vertical antenna patterns together with the vertical array factor gain is calculated as:

$$G^a(\varphi, \theta)[\text{dB}] = G_M^a[\text{dBi}] + G_H^a(\varphi)[\text{dB}] + G_V^a(\theta)[\text{dB}] + G_V^{\text{a,array}}(\theta)[\text{dB}], \quad (5)$$

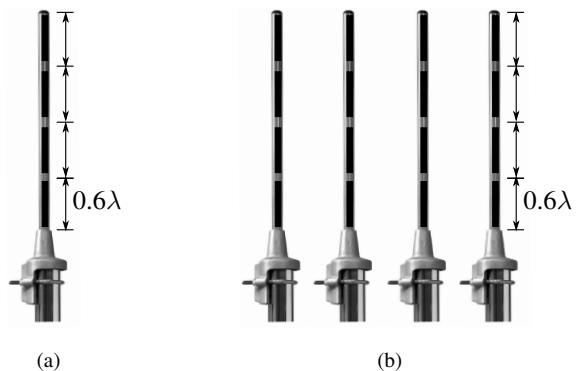


Fig. 18. (a) Vertical half-wave dipole array with four elements spaced by  $0.6\lambda_c$  (b) Horizontal array of vertical half-wave dipoles with four elements spaced by  $0.6\lambda_c$  used for beamforming.

TABLE III  
TYPICAL PARAMETERS OF A DIPOLE ARRAY

Parameter	Value
$N_t$	4
$G_M^a$	2.15 dBi
$d_e$	0.6 wavelength
$a(n)$	[0.97 1.077 1.077 0.86]
$\delta_{\text{phase}}$	1.658 radian

where  $\varphi$  and  $\theta$  are the angles of arrival in the horizontal and vertical planes with respect to the main beam direction, respectively,  $G_M^a$ ,  $G_H^a(\varphi)$  and  $G_V^a(\theta)$  are the maximum antenna gain and the attenuation offsets of one antenna element of the array, respectively, and  $G_V^{\text{a,array}}(\theta)$  is the vertical array factor gain.

The horizontal and vertical attenuation offsets of one antenna element of the array can be respectively modelled as:

$$G_H^a(\varphi)[\text{dB}] = 0, \quad (6)$$

and

$$G_V^a(\theta)[\text{dB}] = 20 \log_{10} \left( \frac{\cos\left(\frac{\pi}{2} \cos\left(\theta + \frac{\pi}{2}\right)\right)}{\sin\left(\theta + \frac{\pi}{2}\right)} \right), \quad (7)$$

while the vertical array factor gain  $G_V^{\text{a,array}}(\theta)$  can be modelled as:

$$G_V^{\text{a,array}}(\theta) = \sum_{n=1}^{N_t} a(n) e^{(j(n-1) \times 2\pi d_e (-\sin(\theta)) + \delta_{\text{phase}})}, \quad (8)$$

where  $N_t$  is the number of antenna elements in the vertical array,  $d_e$  is the spacing between antenna elements in wavelength,  $a(n)$  is the normalised voltage of antenna element  $n$ , and  $\delta_{\text{phase}}$  is the phase increment within antenna elements in radian (see Table III). The horizontal array factor gain in the horizontal plane depends on the beamforming weights used, and those are specified by the used standardised LTE code book beamforming [73].

It is important to note that the proposed configuration was optimised for a given ISD and antenna height, and results in a given certain downtilt. In order to keep the resulting downtilt fixed, the height of the antenna is changed with the ISD. The longer the ISD, the higher the antenna height.

The path gain (loss)  $G_{P,m}$  [dB] represents the gain between a transmitter and a receiver located in this case outdoors for the given environment. The path gain (loss) is modelled as a expected gain value composed of line-of-sight gain, non-line-of-sight gain and a line-of-sight probability as

$$G_{P,m}[\text{dB}] = P_1(d[\text{m}]) \times G_{P_1}(d[\text{m}])[\text{dB}] + (1 - P_1(d[\text{m}])) \times G_{P_n}(d[\text{m}])[\text{dB}]. \quad (9)$$

The line-of-sight probability  $P_1(d[\cdot])$  for a propagation distance  $d$  is based on [67], with an additional spline interpolation for a smooth transition. The resulting line-of-sight  $G_{P_1}(d)$  [dB] and non-line-of-sight  $G_{P_n}(d)$  [dB] path gains for a propagation distance  $d$  are calculated using the 3GPP urban micro (UMi) models [67].  $d$  is computed in the 3D space.

The shadow fading gain (loss)  $G_{S,m}$  [dB] represents the variability of the path loss due to obstruction effects that are not explicitly modelled. The shadow fading gain values are spatially correlated and generated with a log-normal distribution based on [108], [109] with a standard deviation of 6 dB [67]. The inter-small cell BS correlation of shadow fading gain values is 0.5.

The small cell BS transmit power  $P_{\text{tx},m}$  [mW] is calculated to achieve an average targeted SNR at the cell-edge of  $\gamma^{\text{edge}}$  [dB] = 9, 12 or 15 dB as

$$P_{\text{tx},m}[\text{dBm}] = P_N[\text{dBm}] + G_{P,m,\text{edge}}[\text{dB}] + \gamma^{\text{edge}}[\text{dB}]. \quad (10)$$

where  $P_N$  [dBm] is the noise power in dBm, and  $G_{P,m,\text{edge}}$  [dB] is the path gain (loss) from BS  $m$  to its cell-edge, which is  $\frac{\sqrt{3}}{2}$  of the ISD.

The received power from each small cell BS  $m$  at each UE  $u$  is calculated using  $P_{\text{tx},m}$  [mW] and the overall gain  $G_{m,u}$  as

$$P_{\text{rx},m,u}[\text{dBm}] = P_{\text{tx},m}[\text{dBm}] + G_{m,u}[\text{dB}]. \quad (11)$$

The SINR of UE  $u$  when served by small cell BS  $m$  is

$$\gamma_{m,u}[\text{dB}] = \frac{P_{\text{rx},m,u}[\text{mW}]}{\left(\sum_{n=1}^M P_{\text{rx},n,u}[\text{mW}]\right) - P_{\text{rx},m,u}[\text{mW}] + P_N[\text{mW}]}, \quad (12)$$

where  $M$  is the total number of small cell BSs transmitting in the studied frequency band.

From the SINRs and assuming a round robin scheduling, the throughput of UE  $u$  can be calculated as

$$C_u = \frac{C(\gamma_{m,u})}{U}, \quad (13)$$

where  $C(\gamma_{m,u})$  is the SINR to throughput mapping and  $U$  is the number of UEs served by small cell BS  $m$ . The mapping used here is the Shannon-Hartley theorem presented in (1) with an operation point 3.5 dB from the optimum capacity, and there is no cap for the Modulation and Coding Scheme (MCS).

Throughput performance statistics are collected over 150 simulation runs from UEs connected to the small cell BSs in the scenario, with independent UE location and shadow fading realisations. Extra tiers of small cell BSs outside the scenario were added to avoid border effects.

Considering the cell size and the relative proximity of UEs to their serving BSs, there is a high probability of LOS in dense small cell networks, which indicates that Rician fading channel models may be more appropriate than Rayleigh ones to model multi-path channels in this type of deployment. The Rician fading model considers a dominant, non-fluctuating strong path in addition to a number of reflections and scatterings, referred to as LOS and NLOS components, respectively [9].

In the distance dependent multi-path fast fading model used in this paper [63], the  $K$  factor of the traditional Rician model is derived according to the probability of LOS in [67]. This probability of LOS as a function of distance for micro urban scenarios is given as

$$P_{\text{LOS}} = \min\left(\frac{18}{d}, 1\right) \times \left(1 - e^{-\frac{d}{36}}\right) + e^{-\frac{d}{36}}, \quad (14)$$

where  $d$  is the distance between the UE and its serving BS. According to this model, the  $P_{\text{LOS}}$  is equal to 1 within 18 m of the BS, meaning that UEs that are positioned up to 18 m from the serving BS location have a guaranteed strong LOS component.

In order to comply with the  $P_{\text{LOS}}$  of 1, in this distant dependent Rician channel, the value of 32 ( $\sim 15$  dB) is assigned to the  $K$  factor to secure the existence of a strong LOS component within the LOS zone. This value is selected since it results in a standard deviation of the Rician fading smaller than 0.5 dB, flat fading. For UEs locate further away from the BS, the  $P_{\text{LOS}}$  exponentially decays and so does the  $K$  factor due to their one-to-one correspondence. This is modelled by approximating the  $K$  factor,  $K = \frac{P_{\text{LOS}}}{P_{\text{NLOS}}}$ , by an exponentially decaying function. This is interpreted as a distance dependant transition from Rician to Rayleigh fading for UEs that are located further away from their BSs where the LOS component gradually fades.

## REFERENCES

- [1] E. S. Grosvenor and M. Wesson, *Alexander Graham Bell: The Life and Times of the Man Who Invented the Telephone*. Harry N Abrams, Sep. 1997.
- [2] MobiForge, "Global mobile statistics 2014 Part A: Mobile subscribers; handset market share; mobile operators," 2014.
- [3] T. Berners-Lee, *Weaving the Web: The Original Design and Ultimate Destiny of the World Wide Web*. HarperBusiness, Nov. 2000.
- [4] I. McCulloh, H. Armstrong, and A. Johnson, *Social Network Analysis with Applications*. John Wiley & Sons Ltd, Jul. 2013.
- [5] T. Halonen, J. Romero, and J. Melero, *GSM, GPRS and EDGE performance: evolution towards 3G/UMTS*. John Wiley & Sons Ltd, 2004.
- [6] D. Wu, S. Member, Y. T. Hou, W. Zhu, Y. qin Zhang, J. M. Peha, and S. Member, "Streaming video over the Internet: approaches and directions," *IEEE Transactions on Circuits and Systems for Video Technology*, vol. 11, pp. 282–300, 2001.
- [7] E. Setton, T. Yoo, X. Zhu, A. Goldsmith, and B. Girod, "Cross-Layer Design of Ad-Hoc Networks for Real-Time Video Streaming," *IEEE Wireless Communications*, vol. 12, no. 4, pp. 59–65, Aug. 2005.
- [8] Qualcomm, "The 1000x Mobile Data Challenge: More Spectrum, More Small Cells, More Indoor Cells and Higher Efficiency," <http://www.qualcomm.com/>.
- [9] X. Chu, D. López-Pérez, Y. Yang, and F. Gunnarsson, *Heterogeneous Cellular Networks: Theory, Simulation and Deployment*. University Cambridge Press, 2013.
- [10] H. Claussen, L. T. W. Ho, and L. G. Samuel, "An Overview of the Femtocell Concept," *Bell Labs Technical Journal*, vol. 13, no. 1, pp. 221–245, May 2008.

- [11] V. Chandrasekhar, J. G. Andrews, and A. Gatherer, "Femtocell Networks: A Survey," *IEEE Communications Magazine*, vol. 46, no. 9, pp. 59–67, Sept. 2008.
- [12] J. G. Andrews, H. Claussen, M. Dohler, S. Ragan, and M. C. Reed, "Femtocells: Past, present, and future," *IEEE Journal on Selected Areas in Communications (JSAC), Special Issue: Femtocell Networks*, vol. 30, no. 3, pp. 497–508, Apr. 2012.
- [13] 3GPP TR 36.808, "Evolved Universal Terrestrial Radio Access (E-UTRA); Carrier Aggregation; Base Station (BS) radio transmission and reception," 3GPP, Tech. Rep., 2013.
- [14] 3GPP TR 36.889, "Feasibility Study on Licensed-Assisted Access to Unlicensed Spectrum," 3GPP, Tech. Rep., 2014.
- [15] T. S. Rappaport, R. W. H. Jr., R. C. Daniels, and J. N. Murdock, *Millimeter Wave Wireless Communications*. Prentice Hall, 2014.
- [16] L. L. Hanzo, Y. Akhtman, L. Wang, and M. Jiang, *MIMO-OFDM for LTE, WiFi and WiMAX: Coherent versus Non-coherent and Cooperative Turbo Transceivers*. John Wiley & Sons Ltd, 2011.
- [17] M. Ding and L. Hanwen, *Multi-point Cooperative Communication Systems: Theory and Applications*. Springer, 2013.
- [18] Z. Shen, A. Khoryaev, E. Eriksson, and X. Pan, "Dynamic uplink-downlink configuration and interference management in TD-LTE," *IEEE Communications Magazine*, vol. 50, no. 11, pp. 51–59, Nov. 2012.
- [19] M. Ding, D. López-Pérez, W. Chen, and A. Vasilakos, "Dynamic TDD Transmissions in Homogeneous Small Cell Networks," in *IEEE International Conference on Communications (ICC)*, Sydney, Australia, Jun. 2014.
- [20] M. Ding, D. López-Pérez, R. Xue, W. Chen, and A. Vasilakos, "Small Cell Dynamic TDD Transmissions in Heterogeneous Networks," in *IEEE International Conference on Communications (ICC)*, Sydney, Australia, Jun. 2014.
- [21] H. Claussen, I. Ashraf, and L. T. W. Ho, "Dynamic idle mode procedures for femtocells," *Bell Labs Tech. J.*, vol. 15, pp. 95–116, 2010.
- [22] ArrayComm & William Webb, Ofcom, 2007.
- [23] Cisco, "Cisco visual networking index: Global mobile data traffic forecast update, 2014–2019," Global Mobile Data Traffic Forecast Update, 2014-2019," White paper, Feb. 2015.
- [24] A. Damjanovic, J. Montojo, Y. Wei, T. Ji, T. Luo, M. Vajapeyam, T. Yoo, O. Song, and D. Malladi, "A survey on 3GPP heterogeneous networks," *IEEE Wireless Communications Magazine*, vol. 18, no. 3, pp. 10–21, Jun. 2011.
- [25] D. López-Pérez, I. Güvenç, G. de la Roche, M. Kountouris, T. Q. Quek, and J. Zhang, "Enhanced Inter-Cell Interference Coordination Challenges in Heterogeneous Networks," *IEEE Wireless Communications Magazine*, vol. 18, no. 3, pp. 22–31, Jun. 2011.
- [26] Small Cell Forum, "Small Cell Market Status Dec 2012," White paper, Dec. 2012.
- [27] H. Claussen, L. T. W. Ho, and L. G. Samuel, "An overview of the femtocell concept," *Bell Labs Tech. J.*, vol. 13, no. 1, pp. 221–245, May 2008.
- [28] D. López-Pérez, A. Valcarce, G. de la Roche, and J. Zhang, "OFDMA Femtocells: A Roadmap on Interference Avoidance," *IEEE Communications Magazine*, vol. 47, no. 9, pp. 41–48, Sep. 2009.
- [29] D. López-Pérez, X. Chu, and I. Guvenc, "On the Expanded Region of Picocells in Heterogeneous Networks," *IEEE Journal of Selected Topics in Signal Processing (J-STSP)*, vol. 6, no. 3, pp. 281–294, Jun. 2012.
- [30] J. D. Hobby and H. Claussen, "Deployment options for femtocells and their impact on existing macrocellular networks," *Bell Labs Tech. J.*, vol. 13, no. 4, pp. 145–160, Feb. 2009.
- [31] G. de la Roche, A. Valcarce, D. López-Pérez, and J. Zhang, "Access Control Mechanisms for Femtocells," *IEEE Communications Magazine*, vol. 48, no. 1, pp. 33–39, Jan. 2010.
- [32] D. López-Pérez, I. Guvenc, and X. Chu, "Mobility Management Challenges in 3GPP Heterogeneous Networks," *IEEE Communications Magazine*, vol. 50, no. 12, pp. 70–78, Dec. 2012.
- [33] Y.-H. Nam, B. L. Ng, K. Sayana, Y. Li, J. Zhang, Y. Kim, and J. Lee, "Full-Dimension MIMO (FD-MIMO) for Next Generation Cellular Technology," *IEEE Communications Magazine*, vol. 51, no. 6, pp. 172–179, Jun. 2013.
- [34] L. Xie, L. Li, and X. Li, "Sum rate analysis of multicell mu-mimo with 3d user distribution and base station tilting," in *IEEE Vehicular Technology Conference (VTC 2014-Fall)*, Sep. 2014, pp. 1–6.
- [35] B. Priyanto, S. Kant, F. Rusek, S. Hu, J. Chen, and C. Wugengshi, "Robust ue receiver with interference cancellation in lte advanced heterogeneous network," in *IEEE Vehicular Technology Conference (VTC 2013-Fall)*, Sep. 2013, pp. 1–7.
- [36] Y. Xie, H. Zhang, Y. Li, L. Feng, and M. Ji, "Analysis of coverage probability for cooperative heterogeneous network," in *IEEE Vehicular Technology Conference (VTC 2013-Fall)*, Sep. 2013, pp. 1–5.
- [37] H. Wang, C. Rosa, and K. Pedersen, "Analysis of carrier deployment strategies for lte-a hetnets with multicell cooperation," in *IEEE Vehicular Technology Conference (VTC 2014-Fall)*, Sep. 2014, pp. 1–5.
- [38] P. Sorrells, "Wrestling with the Data Tsunami Indoors," White paper, Mar. 2014.
- [39] ETSI MCC, "Draft Report of 3GPP TSG RAN WG1 #77," 3GPP TSG RAN WG1 Meeting #77, Seoul, Korea, Tech. Rep., May 2014.
- [40] H. Ishii, Y. Kishiyama, and H. Takahashi, "A novel architecture for lte-b: C-plane/u-plane split and phantom cell concept," in *IEEE Global Telecommunications Conference (GLOBECOM)*, Dec. 2012, pp. 624–630.
- [41] X. Xu, G. He, S. Zhang, Y. Chen, and S. Xu, "On Functionality Separation for Green Mobile Networks: Concept Study over LTE," *IEEE Communications Magazine*, vol. 51, no. 5, pp. 82–90, May 2013.
- [42] A. Zakrzewska, D. Lopez-Perez, S. Kucera, and H. Claussen, "Dual Connectivity in LTE HetNets with Split Control- and User-Plane," in *IEEE Global Telecommunications Conference (GLOBECOM)*, Dec. 2013, pp. 391–396.
- [43] 3GPP RP 132069, "New Work Item Description: Dual Connectivity for LTE, 3GPP TSG-RAN Meeting 62," 3GPP, Tech. Rep., 2013.
- [44] I. Ashraf, F. Boccardi, and L. Ho, "SLEEP mode techniques for small cell deployments," *IEEE Communications Magazine*, vol. 49, no. 8, pp. 72–79, Aug. 2011.
- [45] R. Razavi and H. Claussen, "Urban Small Cell Deployments: Impact on the Network Energy Consumption," in *IEEE Wireless Communications and Networking Conference (WCNC)*, Paris, France, Apr. 2012.
- [46] W. Wang, P. Ren, Q. Du, and L. Sun, "Robust detection with stable throughput over ill-conditioned channels for high-order mimo systems," in *IEEE Vehicular Technology Conference (VTC 2013-Fall)*, Sep. 2013, pp. 1–5.
- [47] M. Sawahashi, T. Kawamura, and Y. Kakishima, "Csi reference signal multiplexing using carrier frequency swapping for fdd high-order mimo sdm," in *IEEE Vehicular Technology Conference (VTC 2014-Fall)*, Sep. 2014, pp. 1–5.
- [48] A. Sulyman, A. Nassar, M. Samimi, G. MacCartney, T. Rappaport, and A. Alsanie, "Radio propagation path loss models for 5g cellular networks in the 28 ghz and 38 ghz millimeter-wave bands," *IEEE Communications Magazine*, vol. 52, no. 9, pp. 78–86, Sep. 2014.
- [49] T. Rappaport, S. Sun, R. Mayzus, H. Zhao, Y. Azar, K. Wang, G. Wong, J. Schulz, M. Samimi, and F. Gutierrez, "Millimeter wave mobile communications for 5g cellular: It will work!" *IEEE Access*, vol. 1, pp. 335–349, 2013.
- [50] A. Ghosh, T. Thomas, M. Cudak, R. Ratasuk, P. Moorut, F. Vook, T. Rappaport, G. MacCartney, S. Sun, and S. Nie, "Millimeter-wave enhanced local area systems: A high-data-rate approach for future wireless networks," *IEEE Journal on Selected Areas in Communications*, vol. 32, no. 6, pp. 1152–1163, Jun. 2014.
- [51] F. Rusek, D. Persson, B. K. Lau, E. Larsson, T. Marzetta, O. Edfors, and F. Tufvesson, "Scaling Up MIMO: Opportunities and Challenges with Very Large Arrays," *IEEE Signal Processing Magazine*, vol. 30, no. 1, pp. 40–60, Jan. 2013.
- [52] E. Larsson, O. Edfors, F. Tufvesson, and T. Marzetta, "Massive MIMO for Next Generation Wireless Systems," *IEEE Communications Magazine*, vol. 52, no. 2, pp. 186–195, Feb. 2014.
- [53] Qualcomm, "Importance of serving cell selection in heterogeneous networks (R1-100701)," Valencia, Spain, Jan. 2010.
- [54] H.-S. Jo, Y. J. Sang, P. Xia, and J. G. Andrews, "Outage probability for heterogeneous cellular networks with biased cell association," in *IEEE Global Telecommunications Conference (GLOBECOM)*, Houston, TX, Dec. 2011.
- [55] 3GPP TS 36.133, "Evolved Universal Terrestrial Radio Access (E-UTRA); Requirements for support of radio resource management," v.12.6.0, 3GPP, Dec. 2015.
- [56] Alcatel-Lucent, Ericsson, et al., "CR on ABS definition (R2-111701)," Taipei, Taiwan, Feb. 2011.
- [57] I. Güvenç, "Capacity and fairness analysis of heterogeneous networks with range expansion and interference coordination," *IEEE Communications Letters*, vol. PP, no. 99, pp. 1–4, Sep. 2011.
- [58] A. Merwaday, S. Mukherjee, and I. Guvenc, "Capacity analysis of LTE-Advanced HetNets with reduced power subframes and range expansion," *EURASIP Journal on Wireless Communications and Networking*, Nov. 2014.

- [59] S. Deb, P. Monogioudis, and J. M. J. P. Seymour, "Algorithms for Enhanced Inter-Cell Interference Coordination (eICIC) in LTE HetNets," *IEEE/ACM Transactions on Networking*, accepted for publication in a future issue of this journal, 2013.
- [60] B. Soret and K. Pedersen, "Macro Cell Muting Coordination for Non-Uniform Topologies in LTE-A HetNets," in *IEEE Vehicular Technology Conference (VTC Fall)*, Sep. 2013.
- [61] J. Deissner and G. Fettweis, "A Study on Hierarchical Cellular Structures with Inter-Layer Reuse in an Enhanced GSM Radio Network," in *IEEE International Workshop on Mobile Multimedia Communications (MoMuC '99)*, 1999, pp. 243–251.
- [62] I. Ashraf, L. T. W. Ho, and H. Claussen, "Improving energy efficiency of femtocell base stations via user activity detection," in *Proc. IEEE Wireless Communications and Networking Conference (WCNC)*, Sydney, Australia, Apr. 2010.
- [63] A. Jafari, D. Lopez-Perez, M. Ding, and J. Zhang, "Study on Scheduling Techniques for Ultra Dense Small Cell Networks," in *IEEE International Conference on Communications (ICC) Workshops (submitted)*, Jun. 2015, pp. 391–396.
- [64] C. E. Shannon, "A mathematical theory of communication," *Bell System Tech. J.*, vol. 27, pp. 379–423, Jul. 1948.
- [65] J. G. Andrews, F. Baccelli, and R. K. Ganti, "A tractable approach to coverage and rate in cellular networks," *IEEE Transactions on Communications*, vol. 59, no. 11, pp. 3122–3134, Nov. 2011.
- [66] S. Mukherjee, "Distribution of Downlink SINR in Heterogeneous Cellular Networks," *IEEE Journal on Selected Areas in Communications (JSAC)*, vol. 30, no. 3, pp. 575–585, Apr. 2012.
- [67] 3GPP TR 36.814, "Evolved Universal Terrestrial Radio Access (E-UTRA); Further advancements for E-UTRA Physical layer aspects," 3GPP-TSG R1, Tech. Rep. v 1.0.0.
- [68] Y. Kishiyama, A. Benjebbour, T. Nakamura, and H. Ishii, "Future Steps of LTE-A: Evolution Toward Integration of Local Area and Wide Area Systems," *IEEE Wireless Communications*, vol. 20, no. 1, pp. 12–18, Feb. 2013.
- [69] F. Gustafsson and F. Gunnarsson, "Mobile positioning using wireless networks: possibilities and fundamental limitations based on available wireless network measurements," *IEEE Signal Processing Magazine*, vol. 22, no. 4, pp. 41–53, Jul. 2005.
- [70] K. Klessig and V. Suryaprakash, "Spatial Traffic Modelling for Architecture Evolution," Green Touch.
- [71] Z. Pi and F. Khan, "An Introduction to Millimeter-Wave Mobile Broadband Systems," *IEEE Communications Magazine*, vol. 49, no. 6, pp. 101–107, Jun. 2011.
- [72] M. Sanchez-Fernandez, S. Zazo, and R. Valenzuela, "Performance comparison between beamforming and spatial multiplexing for the downlink in wireless cellular systems," *IEEE Transactions on Wireless Communications*, vol. 6, no. 7, pp. 2427–2431, Jul. 2007.
- [73] F. Khan, *LTE for 4G Mobile Broadband: Air Interface Technologies and Performance*. University Cambridge Press, 2009.
- [74] 3GPP TS 36.211, "Evolved Universal Terrestrial Radio Access (E-UTRA); Physical channels and modulation," v.12.2.0, Jul. 2014.
- [75] P. Viswanath, D. N. C. Tse, and R. Laroia, "Opportunistic beamforming using dumb antennas," *IEEE Trans. Inf. Theory*, vol. 48, no. 5, pp. 1277–1294, Jun. 2002.
- [76] C. A. Balanis, *Antenna Theory: Analysis and Design*. John Wiley & Sons Ltd, 2005.
- [77] S. Sesia, I. Toufik, and M. Baker, *LTE: The UMTS Long Term Evolution, From Theory to Practice*. John Wiley & Sons Ltd, Feb. 2009.
- [78] M. Sharif and B. Hassibi, "A comparison of time-sharing, dpc, and beamforming for mimo broadcast channels with many users," *IEEE Transactions on Communications*, vol. 55, no. 1, pp. 11–15, Jan. 2007.
- [79] T. Bu, L. Li, and R. Ramjee, "Generalized proportional fair scheduling in third generation wireless data networks," in *25th IEEE International Conference on Computer Communications (INFOCOM)*, Apr. 2006, pp. 1–12.
- [80] E. Liu and K. Leung, "Proportional fair scheduling: Analytical insight under rayleigh fading environment," in *IEEE Wireless Communications and Networking Conference (WCNC)*, Mar. 2008, pp. 1883–1888.
- [81] G. Mongha, K. Pedersen, I. Kovacs, and P. Mogensen, "QoS Oriented Time and Frequency Domain Packet Schedulers for The UTRAN Long Term Evolution," in *IEEE Vehicular Technology Conference, 2008.*, May 2008, pp. 2532–2536.
- [82] A. Jalali, R. Padovani, and R. Pankaj, "Data throughput of cdma-hdr a high efficiency-high data rate personal communication wireless system," in *IEEE 51st Vehicular Technology Conference (VTC 2000-Spring)*, vol. 3, 2000, pp. 1854–1858 vol.3.
- [83] H. Claussen, "Future Cellular Networks," Alcatel-Lucent, Apr. 2012.
- [84] B. D. Claude Dessel and F. Louagie, "Flexible Power Model of Future Base Stations: System Architecture Breakdown and Parameters," Green Touch.
- [85] D. O'Donoghue, V. Nico, R. Frizzell, G. Kelly, and J. Punch, "A multiple-degree-of-freedom velocity-amplified vibrational energy harvester: Part a — experimental analysis," *Proceedings of the American Society of Mechanical Engineers*, vol. 2, Sep. 2014.
- [86] V. Nico, D. O'Donoghue, R. Frizzell, G. Kelly, and J. Punch, "A multiple degree-of-freedom velocity-amplified vibrational energy harvester: Part b — modelling," *Proceedings of the American Society of Mechanical Engineers*, vol. 8, Sep. 2014.
- [87] K. Divya and J. Oestergaard, "Battery Energy Storage Technology for Power Systems — an Overview," *Electric Power Systems Research J.*, vol. 79, no. 4, pp. 511–520, 2009.
- [88] C. Nicoll, "3G and 4G Small Cells Create Big challenges for MNOs," Analysis Mason, Mar. 2013.
- [89] "SCF049: Backhaul technologies for small cells (Release 4)s," Small Cell Forum, Feb. 2014.
- [90] U. Gustavsson, C. Sanchez-Perez, T. Eriksson, F. Athley, G. Durisi, P. Landin, K. Hausmair, C. Fager, and L. Svensson, "On the Impact of Hardware Impairments on Massive MIMO," in *IEEE Global Telecommunications Conference (GLOBECOM)*, Austin, Texas, Dec. 2014.
- [91] J. Jose, A. Ashikhmin, T. Marzetta, and S. Vishwanath, "Pilot Contamination and Precoding in Multi-Cell TDD Systems," *IEEE Transactions on Wireless Communications*, vol. 10, no. 8, pp. 2640–2651, Aug. 2011.
- [92] K. T. Truong and J. R. W. Heath, "Effects of Channel Aging in Massive MIMO Systems," *Journal of Communications and Networks, Special Issue on Massive MIMO*, vol. 15, no. 4, pp. 338–351, Aug. 2013.
- [93] L. Chun-Hung and X. Feng, "Network Coding for Two-Way Relaying: Rate Region, Sum Rate and Opportunistic Scheduling," in *IEEE International Conference on Communications (ICC)*, May 2008, pp. 1044–1049.
- [94] L. Huaping, P. Popovski, E. de Carvalho, Y. Zhao, and F. Sun, "Four-way relaying in wireless cellular systems," *IEEE Wireless Communications Letters*, vol. 2, no. 4, pp. 403–406, Aug. 2013.
- [95] J. Puttonen, N. Kolehmainen, T. Henttonen, and J. Kaikkonen, "On idle mode mobility state detection in evolved UTRAN," in *Proc. IEEE International Conference on Information Technology: New Generations*, Las Vegas, NV, Apr. 2009, pp. 1195–1200.
- [96] 3GPP TR 36.842, "Study on Small Cell Enhancements for E-UTRA and E-UTRAN; Higher layer aspects," v.12.0.0, Jan. 2014.
- [97] H. Claussen, L. T. W. Ho, and L. G. Samuel, "Financial analysis of a pico-cellular home network deployment," in *Proc. IEEE International Conference on Communications (ICC)*, Glasgow, UK, June 2007, pp. 5604–5609.
- [98] H. Claussen, L. T. W. Ho, and F. Pivit, "Self-optimization of femtocell coverage to minimize the increase in core network mobility signalling," *Bell Labs Tech. J.*, vol. 14, no. 2, pp. 155–184, Aug. 2009.
- [99] R. Razavi, L. Ho, H. Claussen, and D. Lopez-Perez, "Improving Small Cell Performance through Switched Multi-element Antenna Systems in Heterogeneous Networks," *IEEE Transactions on Vehicular Technology*, vol. PP, no. 99, pp. 1–1, 2014.
- [100] M. Amirjoo, P. Frenger, F. Gunnarsson, H. Kallin, J. Moe, and K. Zetterberg, "Neighbor Cell Relation List and Physical Cell Identity Self-Organization in LTE," in *IEEE International Conference on Communications (ICC)*, May 2008, pp. 37–41.
- [101] G. Sun, J. Chen, W. Guo, and K. Liu, "Signal processing techniques in network-aided positioning: A survey of state-of-the-art positioning designs," *IEEE Signal Processing Magazine*, vol. 22, no. 4, pp. 12–23, Jul. 2005.
- [102] ETSI MCC, "Draft Report of 3GPP TSG RAN WG1 #75," Tech. Rep., Nov. 2013.
- [103] 3GPP TR 36.828, "Further enhancements to LTE Time Division Duplex (TDD) for Downlink-Uplink (DL-UL) interference management and traffic adaptation," v.11.0.0, Jun. 2012.
- [104] M. Ding, D. López-Pérez, W. Chen, and A. Vasilakos, "Analysis on the SINR Performance of Dynamic TDD in Homogeneous Small Cell Networks," in *IEEE Global Telecommunications Conference (GLOBECOM)*, Austin, Texas, Dec. 2014.
- [105] A. Cavalcante, E. Almeida, R. Vieira, F. Chaves, R. Paiva, F. Abinader, S. Choudhury, E. Tuomaala, and K. Doppler, "Performance Evaluation of LTE and Wi-Fi Coexistence in Unlicensed Bands," in *IEEE Vehicular Technology Conference (VTC Spring)*, Jun. 2013, pp. 1–6.
- [106] ETSI MCC, "Draft Report of 3GPP workshop on LTE in unlicensed spectrum," 3GPP workshop on LTE in unlicensed spectrum, Sophia Antipolis, France, Tech. Rep., Jun. 2014.

- [107] H. Claussen and L. T. W. Ho, "Multi-carrier Cell Structures with Angular Offset," in *IEEE Personal, Indoor and Mobile Radio Communications (PIMRC)*, Sydney, Australia, Sept. 2012, pp. 1–6.
- [108] M. Gudmundson, "Correlation model for shadow fading in mobile radio systems," *Electron. Lett.*, vol. 27, no. 2, pp. 2145–2146, Nov. 1991.
- [109] H. Claussen, "Efficient modelling of channel maps with correlated shadow fading in mobile radio systems," in *Proc. IEEE Int. Symp. Personal, Indoor and Mobile Radio Commun. (PIMRC)*, Berlin, Germany, Sept. 2005, pp. 512–516.